

LIBRARY Michigan State University

This is to certify that the dissertation entitled

PROTON TRANSFER REACTIONS IN DIHYDROGEN BONDED SYSYEMS

presented by

SIMONA MARINCEAN

has been accepted towards fulfillment of the requirements for the

Ph.D.	degree in _	ORGANIC CHEMISTRY
	Major Profe	essor's Signature
	08	3.11.2003 Date

PLACE IN RETURN BOX to remove this checkout from your record. TO AVOID FINES return on or before date due. MAY BE RECALLED with earlier due date if requested.

DATE DUE	DATE DUE	DATE DUE

6/01 c:/CIRC/DateDue.p65-p.15

PROTON TRANSFER REACTIONS IN DIHYDROGEN BONDED SYSTEMS

By

Simona Marincean

A DISSERTATION

Submitted to

Michigan State University

in partial fulfillment of the requirements

for the degree of

DOCTOR OF PHYLOSOPHY

Department of Chemistry

2003

ABSTRACT

PROTON TRANSFER REACTIONS IN DIHYDROGEN BONDED SYSTEMS

By

Simona Marincean

As possible substrates for one-photon infrared-pumped reaction (IRPR), the structures and decomposition paths of complexes between AlH₄⁻ and three proton donors, H₂O, HF, and HCl, have been studied by ab initio methods at the MP2//6-311++G** level of theory. Dihydrogen bonded complexes, [AlH₄...HA]⁻ (A=OH, F, Cl), were obtained as minima on the potential energy surface (PES). In each case only one transition state was found for the proton transfer and H₂ loss process. For each cluster, the geometry and energy characteristics of reactants, complex, transition state, and products were analyzed with [AlH₄...HCl]⁻ emerging as the best IRPR candidate. The calculated intrinsic reaction coordinate (IRC) confirmed the one-step proton transfer and H₂ loss with no intermediate. Classical trajectories for the vibrationally activated process were calculated on the ab initio potential energy surface, beginning with varying degrees of excitation of the modes associated with proton transfer, 1411 and 1973 cm⁻¹. Proton

transfer from HCl and loss of H_2 were calculated to occur on the femtosecond time scale for several of the initial conditions, including the first vibrationally excited level.

The influence of the dihydrogen bonding on the activation parameters of ketone reduction by tetrabutyl ammonium borohydride, NBu₄BH₄, has been studied. 2-Hydroxycyclopentanone was chosen as substrate because it was the most thoroughly studied in the previous works in this group. The reaction kinetics were found to be first order in ketone and in borohydride with a rate constant of k=2.20 \pm 0.160 x 10⁻³ l·mol⁻¹·s⁻¹ at room temperature. Formation of a dihydrogen bonding complex between the hydroxyl substituent and the BH₄ lowered the activation enthalpy by 6.6 kcal/. Comparison of the activation entropy for the 2-hydroxycyclopentanone and cyclopentanone reductions, -29.6 and -22.9 e.u. respectively, pointed to a higher organization degree in the transition state when the substrate bears an α-hydroxyl group. When a hydrogen bonding solvent was used the activation parameters were lowered even more as expected, due to increase number of proton donor partners. Direct analysis of the products ratio showed a smaller stereochemical control than reported previously. The influences of different factors on the stereochemical outcome are discussed.

TABLE OF CONTENTS

LI	ST OI	F TABLES	v
LI	ST OI	F FIGURES	vi
1.	Lite	rature Review	1
	1.1.	Selective Bond Dissociation via Photon Excitation	1
	1.2.	IR Laser Pump Spectroscopy in Hydrogen Bonded Systems	12
	1.3.	Dihydrogen Bonding	26
	1.4.	Proton Transfer in Dihydrogen Bonded Systems	37
2.	Dyn	amic Studies for Proton Transfer in Dihydrogen-bonded	
	Con	aplexes involving AlH4 ⁻	56
3.	Kin	etic and Mechanistic Investigations of 2-Hydroxycyclopenta	none
	Rec	luction by Borohydride	74
4.	Met	thods of Calculation	90
5.	Exp	perimental Section	94
B	IBLY	OGRAPHY	98

LIST OF TABLES

Table 5.1 Dihydrogen Bonded Complexes: Geometries	62
Table 5.2 Energetics of Proton Transfer Reaction for Dihydrogen Bond	led
Complexes	63
Table 6.1. Reported Reduction Results of α-Hydroxycycloalkanones as	nd of
Corresponding Unsubstituted Ketones	76
Table 6.2. Rate Constants for the Reduction of	
2-Hydroxycyclopentanone by NBu ₄ BH ₄	81
Table 6.3. Activation Parameters for Ketones Reductions	83
Table 6.4 Work-up Procedures Results	84
Table 6.5 Trans: Cis Ratios in 2-Hydroxycyclopentanone Reduction	86

LIST OF FIGURES

Figure 2.1 OH Frequencies for EtOH Oligomers in CCl ₄ 13
Figure 2.2 Laenen Model for EtOH Excitation
Figure 2.3 Bakker Model for the OH Excited Mode20
Figure 2.4 10M NaOD Solution in D ₂ O22
Figure 3.1 Dihydrogen Bonded Complex26
Figure 3.2 Alane Piperidine Adduct29
Figure 3.3 Cyclotrialumazane30
Figure 3.5 $[Ir(PMe_3)_4(H)(OH)]^+$ and $[Fe(H)_2(H_2)(PEt_2Ph)_4]$
Complexes31
Figure 3.6 Bifurcated Hydrogen Bonds in Ir Hydride Complexes34
Figure 3.7 Dihydrogen Bonds in W Hydrides Complexes35
Figure 4.1 NH4 Structures
Figure 4.2 Proton Transfer in the H ₃ O Complex39
Figure 5.1 [AlH ₄ H ₂ O] Complex Structures: Reactant, Transition State,
and Products59
Figure 5.2 [AlH ₄ HF] Complex Structures: Reactant, Transition State, and
Products60
Figure 5.3 [AlH ₄ HCl] Complex Structures: Reactant, Transition State,
and Products61

Figure 5.4 IRC Calculation for Proton Transfer and H ₂ Loss in
[AlH4HCl] ⁻
Figure 5.5 Excited Modes66
Figure 5.6. Distance Evolution in Vibrationally Excited Complex at 1411
cm ⁻¹ 68
Figure 5.7 H(1)-H(2) Distance Evolution in Vibrationally Excited Complex
at 1973 cm ⁻¹ 70
Figure 5.8 Evolution of the 1411 and 1973 cm ⁻¹ Modes Upon Transition
State Relaxation71
Figure 5.9 Evolution of the Modes Other Than 1411 and 1973 cm ⁻¹ Upon
Transition State Relaxation72
Figure 6.1 Time Evolution of Ketone Concentration80
Figure 6.2 Time Evolution of Borohydride Concentration80
Figure 6.3 Integrated Rate Laws for Reduction of
2- Hydroxycylopentanone by NBu ₄ BH ₄ 81
Figure 6.4 Logarithmic Representation of the Eyring Equation82
Figure 6.5 2-Hydroxycyclopentanone87
Figure 6.6 2-Hydroxycyclopentanone·BH ₄ Complexes87

1. Literature Review

1.1 Selective Bond Dissociation via Photon Excitation

There are two main ways to achieve excitation of molecules in order to activate them for reaction. The most familiar distributes kinetic energy via thermal activation raising a fraction of the molecules above the activation barrier, as dictated by the Boltzman distribution. The second way is to supply external energy by a mechanism that is "not subject to the equilibrium distribution law of canonical ensembles". Chemical activation, single/multi photon excitation, collisions in molecular beams, and photosensitization reactions can accomplish the latter. This thesis probes the behavior of such-nonequilibrium excitations in the recently popular dihydrogen bonded systems.

The notion of selective bond cleavage via vibrational activation

("molecular scissors") has long been recognized as a natural corollary to the identification of infrared absorption bands with molecular functional groups. In principle, deposition of sufficient vibrational energy into a chemical bond's stretching mode should induce its rupture, resulting in an infrared-pumped reaction (IRPR). But many vibrational quanta are needed to break a typical bond, so this idea was not seriously considered until the

advent of pulsed lasers, light sources intense enough to accomplish rapid multiphoton excitation.²

Unfortunately, though lasers have been crucial in the development of today's understanding of molecular dynamics, the main result is the knowledge that the timescales for multiphoton absorption and, most importantly, for vibrational relaxation are typically much faster than for any intended reaction. Early measurements showed that intramolecular vibrational relaxation takes places on a picosecond time scale. The challenge to those who would design IRPRs is thus clear: the reaction time must be competitive with the relaxation time of the vibrational mode in question; the energy deposited must of course be adequate to surmount the activation barrier (including thermal and tunneling contributions) for the process; and the overall reaction should be irreversible or at least exothermic (i.e. the back reaction should have a high barrier).

Zewail pointed out that vibrational relaxation takes place via two modes: energy dedistribution and phase loss, and it is important to know their respective contributions to the apparent relaxation processes as criteria for tuning of laser pulse shape and duration.² Experiments done by exciting C-H stretches in naphthalene found relaxation times under around 0.1 ps pointing up the need for subpicosecond lasers.³ Zewail also made the point

of differentiating between the vibrational modes of interest, i.e. the ones to be excited, and the other modes that are not excited directly but interact with the first ones and that can function as energy sinks.

Early attempts of laser control of reactions are characterized by multiphoton excitation. King et al. induced reactions in tetrazine in neat and mixed crystals at low temperature (**Scheme 1.1**). Isotopic composition in the products was controlled by tuning the laser to absorption band of the molecule with a specific isotope component.⁴

Scheme 1.1

$$\begin{array}{c|c}
N & \hline
 & hv \\
\hline
 & 1.6 \text{ K}
\end{array}$$
N₂ + HCN

The reaction takes place from the electronic excited states and exhibits molecular selectivity but showed that lasers could drive reactions.

Multiphoton excitation of terminal and non-terminal olefinic C-H stretches in CH₂=CH-CH₂-NC induced isomerization,⁵ which was explained by a reaction time much faster than IVR in this particular case (Scheme 1.2).

Scheme 1.2

$$CH_2=CH-CH_2-NC \longrightarrow CH_2=CH-CH_2-CN$$

Isomerization and fragmentation were obtained via multiphoton excitations of the CH₂ stretch and wag vibrations in cyclopropane in the gas phase.⁶

Products were the same as resulted from thermal excitation (Scheme 1.3) but their distribution was different. Excitation of the CH₂ wag favored the isomerization path.

Scheme 1.3

$$\begin{array}{ccc} & \longrightarrow & \text{CH}_2\text{=CH-CH}_3 \\ \\ & \longrightarrow & \text{CH}_2\text{=CH}_2 + : \text{CH}_2 \end{array}$$

In a nice review about IR-laser chemistry, Quack et al., referring to mode selective excitation, cautioned that different reactive populations will be induced by excitation via laser as opposed to chemical or thermal activation or by different excitation frequencies and therefore different products distributions which are "no proof whatsoever for mode selective reaction control". In an attempt to use different chromophores to probe the mode selective excitation they used F-CH₂-CH₂-CH₂-CH_D-F but no mode selectivity was observed (Scheme 1.4).

Scheme 1.4

Among theoretical approaches to actively control product formation in a reaction, of major impact are work done by Rice et al., Brumer and Shapiro, and Rabitz et al. Rice suggested that selection control of the products in a branching reaction could be achieved by transfer of vibrational amplitude from ground state to an excited state and, after a specific time delay, back to ground state. Gerber et al. applied this formalism for the ionization and dissociative ionization of Na₂ and demonstrated control of different product channels, (Scheme 1.5), by choosing the selective delay time between pump and control laser pulses.⁸

Scheme 1.5

$$Na_2 \longrightarrow Na_2^* \longrightarrow Na_2^+ + e^-$$

$$\longrightarrow Na + Na^+ + e^-$$

An improved version, the Tannor-Rice method, used the phase to control the reaction outcome in addition to the original pump-dump delay. If

previously the transfer from the excited state to the ground state was not affected by phase, now the phase was locked to that of the pump pulse and therefore interference occurred. Scherer studied this method experimentally in generating fluorescence-detected dynamics of I₂.

Brummer and Shapiro used an approach that relied on the fact that a molecule at an energy where dissociation is possible is characterized by a continuum of degenerate eigenstates. 10-12 Control over the probability of a desired product quantum state was obtained by producing a linear combination of these degenerate states. They chose to take advantage of the interference between amplitudes of different states that connect the reactants and products. Gordon et al. applied this method in studying the ionization and dissociation of HI and DI by one and three-photon excitation and they showed that the phase difference between the ionization and dissociation products is dependent on the excitation energy. 13, 14

A more sophisticated version of this approach, called "incoherent interference", considers that a single field transfers population from ground state to the degenerate target states. ^{15, 16} A second pulse will connect the final states to another empty state. Provided the fields are strong enough they will interfere and control can be obtained by tuning the interference.

Brumer and Shapiro found out that efficiency is at a maximum when the pulse relative to the target states is applied before the excitation pulse but overlapping with it. This method is called stimulated Raman adiabatic passage (STIRAP) and Kobrak and Rice developed an extended version of it that allows for product selectivity in a chemical reaction. ^{17, 18} Experimental work to confirm this approach has been done by Shnitman in proving laser control over a branching photochemical dissociation of Na₂ (Scheme 1.6). Control was demonstrated over the Na(3d), Na(3p) branching ratio by using a two-photon incoherent interference scenario based on pump and dump laser pulses with variable frequencies. ^{19, 20}

Scheme 1.6

$$Na_2 \longrightarrow Na (3s) + Na (3p)$$

$$\longrightarrow Na (3s) + Na (4s)$$

$$\longrightarrow Na (3s) + Na (3d)$$

Recently Abrashkevich et al. studied computationally the possibility of control over dissociation of collinear CH₂BrI to yield either CH₂Br +I or CH₂I + Br. The authors reported that the control level depends strongly on the superposition created by the first step excitation that was achieved with experimentally controllable laser amplitudes and phases.²¹

The Hamiltonian at the Born-Oppenheimer level remains unknown for polyatomic molecules. A method of closed loop control introduced by Rabitz offers a way to surmount this problem in finding the appropriate laser pulse. This theoretical concept is denoted by optimal control theory, (OCT). The goal of OCT is to design an electric field that allows for desired manipulation of the system. An important feature is the competition between the maximization of the expectation value of an observable and the constraints imposed by the electric field. All the objectives are included in the cost functional which is optimized with respect to the electric field in such a way that it yields best possible control performance. Although the OCT simulations had to be carried out on simple systems due to computational cost, they showed that successful control fields are possible.

Related to OCT are optimal control experiments, OCE, based on adaptive control techniques and Rabitz et al. have suggested them.²⁴⁻³⁰

In this approach a loop is closed around the system, observables are used to refine the candidate laser field applied until the control objective is achieved as best possible. The elements involved are: an input laser design, the apparatus needed to generate the laser pulses, application of the laser field to the quantum system, observation of the control outcome, and a learning algorithm that analyzes the results of the prior experiments and suggests a

new control field. The advantage by comparison with OCT resides in the ability of the system to "solve its own Schrodinger equation".

Selective bond dissociation has been achieved in a series of ketones.³¹ Starting out with acetone it has been demonstrated that optimizations to the point where one pathway can be favored over the other can be achieved in a reasonable laboratory time, 10 min, and also that strong fields are able to alter the relative ion yields and therefore the information content in the mass spectrum which is used to measure the control observable. The control over selective bond cleavage was studied with trifluoroacetone and acetophenone. In the first case the dissociation pathways are not identical, (Scheme 1.8) and indeed CF₃ signal was enhanced compared to the initial one but not at the expense of suppressing other pathways, i.e. the CH₃ branch.

Scheme 1.8

$$CH_3$$
-CO-CF₃ \rightarrow CH_3 -CO + CF₃
 \rightarrow CF₃-CO + CH₃

For acetophenone one pathway was favored over another in contrast with the dissociation energy (preferential cleavage of the phenyl ring was obtained even though the energy required to cleave the Ph-CO bond is 15 kcal /mol higher than that for CH₃-CO bond). Also a rearrangement pathway was observed and limited control over it was achieved (c, Scheme 1.9).

Scheme 1.9

Using the same method Gerber showed control over different dissociation pathways in organometallic compounds.³² Gerber demonstrated the possibility of adaptive control in the liquid phase when 4-dicyanomethylene-2-methyl-6-p-dimethylaminostyryl-4H-pyran was excited selectively over [Ru(dpb)₃](PF₆)₂ (dpb is 4,4'-diphenyl-2,2'-bipyridine) when both compounds were dissolved in methanol.³³

All the control experiment approaches are based on multiphoton laser excitation in the UVE domain. As one can see from the examples given the reactions that are subjected to investigation are unimolecular. The limitations arise from that fact that UV spectroscopy is not functionality specific and also the majority of reactions of interest for chemists are at least

bimolecular. In bimolecular reactions two features add to the complexity of the problem: orientation of the reactants, and collisions.³⁴

Althorpe et al. studied the mechanism of the $D_2 + H \rightarrow D + HD$ reaction, using multiphoton excitation. They reported two mechanisms to take place, the dominant one is characterized by scattering of the newly formed HD molecule in the opposite direction than the initial approach of the H atom. The second mechanism, which is observed with a 25 fs delay, ejects the HD molecule in the same direction as the initial approach.³⁵

1.2. IR Laser Pump Spectroscopy in Hydrogen Bonded Systems

Infrared laser spectroscopy allows for time-resolved studies of vibrational dynamics. General principle is to excite with a laser pulse the bond of interest and with a second delayed pulse to probe the dynamics of the system. Hydrogen bonded complexes have been studied due to their importance in modern chemistry and biology and because little is known about their structure and dynamics.

Heiweil et al. were the first ones to use IR pump-probe spectroscopy investigate monomeric EtOH in CCl₄, (<0.007 mole fraction). They bleached the OH frequency and monitored its recovery with a 20 ps laser pulse tuned to 3625 cm^{-1} and reported a dissociation time of $70 \pm 10 \text{ ps.}^{36}$

Graner, Ye and Laubereau performed classical IR spectroscopy on different concentration solutions of EtOH in CCl₄, and they concluded that internal hydrogen bonds were responsible for a peak at 3300 cm⁻¹. ³⁷⁻³⁹ Excitation of a 0.42 M solution with a 10 ps laser at this frequency followed by a probe pulse at different delay times allowed for study of hydrogen bonds dynamics. The excitation energy exceeded the strength of the hydrogen bond in EtOH, which was determined to be 6 kcal/mol, ^{40, 41} and thus cleavage was achieved. The dissociation was faster than the duration of the laser pulse and therefore its time constant could not be determined while

the recovery of the hydrogen bonds had a time constant of 20 ± 5 ps. Careful examination of the signal curve and of the transmission increase led the authors to conclude that the absorption onset is delayed by 5 ± 3 ps, which they labeled "predissociation lifetime", i.e. lifetime of the excited molecules before dissociation. Cleavage of hydrogen bonds was considered to be an efficient relaxation channel.

Hole-burning spectroscopy is techniques that typically bleaches a spectral band of a molecule and provides information about the vibrational levels of the molecule. IR hole-burning spectroscopy started with the availability of the IR lasers. Laenen and Labereau used this technique to study EtOH solutions in CCl₄ using a laser with an excitation pulse of 2 ps and a probe pulse of 1 ps.⁴² At 1.2 M concentration of EtOH, oligomers present are characterized as expected by specific peaks, **Figure 2.1**.

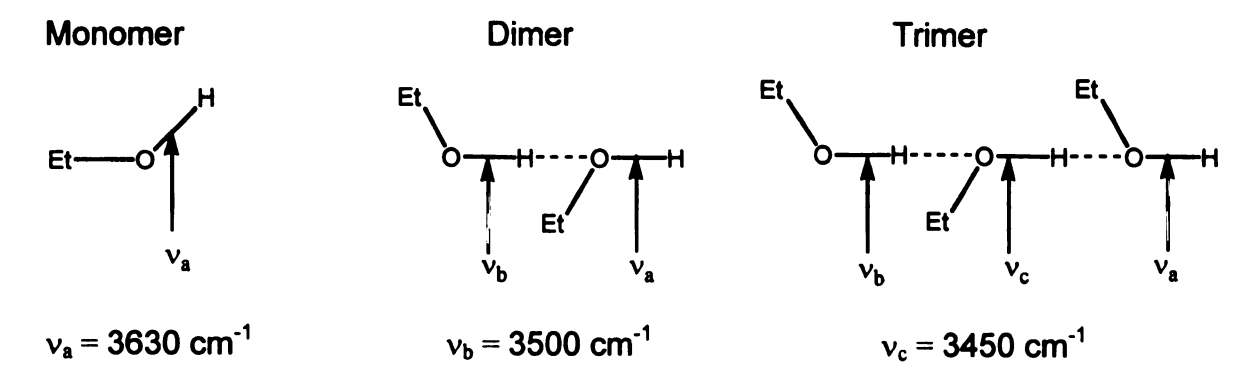


Figure 2.1 OH Frequencies for EtOH Oligomers in CCl₄

EtOH trimers, tetramers/pentamers, and larger polymers are characterized by stretching vibrations of internal OH groups at 3450, 3330, and 3240 cm-1, respectively.⁴³

Upon excitation of the internal OH groups, Laenen et al. demonstrated transient hole burning with a lifetime of 1 ps, estimated from relative transmission change as a function of the delay time. The spectral holes were attributed to transitions from ground state (0) to the first excited vibrational level (1). Bleaching that was observed at early delay times, -2 ps, persisted for long times, >80 ps, and was considered evidence for rapid spectral relaxation and/or vibrational energy redistribution of the OH groups. Also induced absorption was reported on the red excitation frequency at early delay times as a result of excited state absorption (ESA) from first to second excited levels of the OH-stretching mode. At longer delay time, 5 ps, an induced absorption in the blue wing of the excitation frequency illustrated the formation of smaller hydrogen bonded oligomers as a result of hydrogen bonds breaking. In order to deduce quantitative information from the measured spectra a five states model was proposed, Figure 2.2.

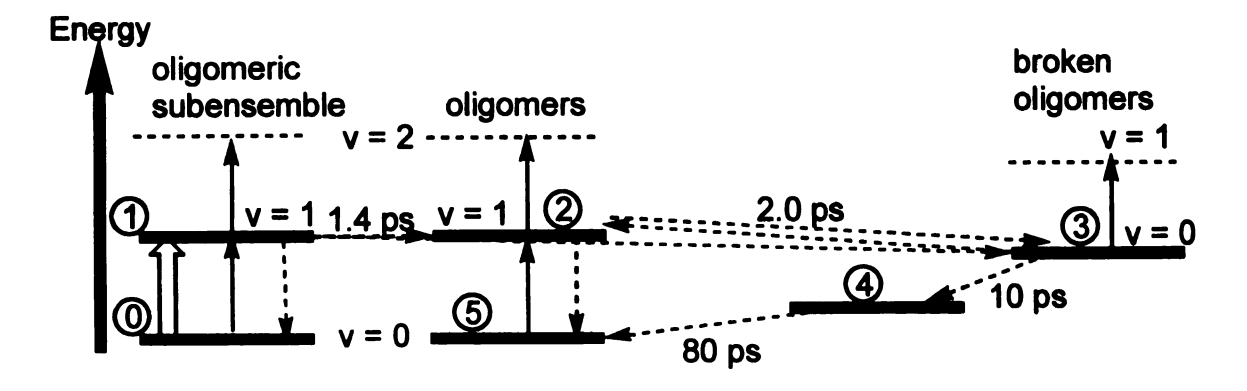


Figure 2.2 Laenen Model for EtOH Excitation

The short intense pulse at 3330 cm⁻¹, indicated by the thick arrow, produced transitions to the first excited vibrational level (state 1), which was observed as a transient spectral hole. The excited subensemble of oligomers relaxed via spectral redistribution and/or energy transfer to a larger ensemble while maintaining the population of the vibrational excited state (state 2). Because the excitation energy exceeded the hydrogen bond energy, dissociation could be considered an important decay channel for the vibrational excitation with formation of smaller oligomers observed in the spectrum, (state 3). Reassociation involved local temperature changes leading to a nonequilibrum distribution of hydrogen bonds at a higher temperature, (state 4), followed by thermalization, (state 5). The probing transitions are indicated by thin arrows and the relaxation pathways by dashed arrows. ESA was considered a direct measure of the excited state population, generated by the pump pulse. The time constant deduced from the corresponding

signal transient (relative transmission change as function of delay time for pulse at 3330 cm^{-1} and probe at 3100 cm^{-1}) was consequently interpreted as the population lifetime and determined to be 1.4 ± 0.3 ps. The difference between the hole and the population lifetime was explained as a result of structural changes around the individual excited OH groups and /or vibrational energy transfer to neighboring EtOH molecules. Computations of transient spectra for different delay times using the proposed model and comparison with the experimental results led to a dissociation time of 2.0 ps. The reassociation was much slower, 10 ps.

At a lower concentration, 0.17 M EtOH in CCl₄, new features about the hydrogen bond dynamics were observed.⁴⁴ At this concentration, monomer and dimer bands are observed at 3633 and 3500 cm⁻¹, respectively. Excitation in the same oligomer region, at 3350 cm⁻¹, induced again transient holes with a lifetime of 1.2 ps and ESA with 1.7 ps. Spectral relaxation via energy migration along the hydrogen bonded chain was found to be fast. Breaking of hydrogen bonds was a very effective relaxation channel with a quantum yield of 0.9. Reassociation occurred on a much longer scale, 23 ps. As expected at 0.05 M EtOH in CCl₄, when only monomers are observed, the lifetime of the excited state is 8 ps,⁴⁵ five times longer than the one corresponding to 0.17 M solution.

Bakker et al. also investigated EtOH solution in CCl4 with a concentration of 1.2 M, using a femtosecond laser (100 fs, 1 mJ).⁴⁶ Upon excitation of the oligomer band at 3330 cm⁻¹, they noted that the relaxation had two components: a fast one, with a constant of 250 fs, and a slower decay at a transmission value that was slightly higher then the initial one, with a time constant of 15 ps. Excitation at different frequencies showed the same pattern with an increase of the predissociation lifetime up to 900 fs when the excited frequency was 3450 cm⁻¹. This dependence on excitation frequency proved the inhomogeneous character of hydrogen bonds and also that the predissociation rate is influenced by the hydrogen-bond strength. In the model that the authors proposed for the process, the excitation of the O-H stretch vibration is followed by a fast delocalization over the hydrogen bonded oligomer and breaking of hydrogen bonds.

Early studies of MeOH oligomers in a N₂ matrix showed that upon irradiation in the mid-IR cyclic trimers could be transformed in open chains and also that this conversion could be reversed by increasing the temperature.⁴⁷ Also work done by Bakker et al. on both MeOH dissolved in CCl₄ and MeOH in zeolites, showed that excitation of internal OH stretch vibrations led to dissociation that was faster then the duration of the laser pulse (18 ps).⁴⁸ Calculations to fit the data led to time constants of 0.5 and

10 ps for solution and zeolites, respectively. The reassociation time for both cases was so much larger that in the zeolites it was outside the experimentally measurable range. The argument was that the solvent keeps the dissociated partners in close proximity by a cage effect while in zeolites that arrangement is not likely since in the zeolites experiments the methanol concentration was kept well below complete saturation of the zeolite.

Applying a new technique, 3D IR-Raman spectroscopy, Dlott et al.⁴⁹ investigated the vibrational energy relaxation in neat methanol at room temperature. 3D IR-Raman spectroscopy uses resonant vibrational pumping by a tunable mid-IR pulse and incoherent anti-Stokes Raman probing. The first two dimensions were represented by a series of incoherent anti-Stokes Raman spectra at a given mid-IR pump frequency, and the third dimension involved changing the IR pump frequency within the range of CH and OH stretching transitions. The authors reported no observation of nonassociated MeOH transition created by vibrational predissociation as a result of OH stretch pumping, but they stressed the point that the experiments were done on neat MeOH in which the molecules are involved in large hydrogenbonded networks and essentially all molecules have multiple hydrogen bonds. The instantaneous generation of OH bending (1380 cm⁻¹) transients when the OH stretch (3250 cm⁻¹) was pumped was considered evidence of

vibrational predissociation. Interestingly they also noted that even though the OH mode is not directly coupled to the C-H stretch, excitation of the methyl-rocking mode together with a significant population of the C-O stretch mode is present.

In contrast with Bakker's and Laenen's work, the Fayer group showed that excitation of OD non-donating groups in MeOH dissolved in CCl₄ with a laser pulse tuned to 2690 cm⁻¹ led to dissociation with a time constant of 2 ps proving that relaxation does not have to be necessarily in the excited O-H...O stretch.⁵⁰ More work on deuterated alcohols, MeOD, EtOD, and PrOD, from the same group led to dissociation times of 2-3 ps upon excitation of non-donating OD groups. The mechanism was rationalized in terms of sequential hydrogen bond dissociation via intramolecular energy redistribution followed by energy transfer into the intermolecular modes.⁵¹ When they measured the OD relaxation of groups that both donate and accept hydrogen bonds in a MeOD solution in CCl₄ both mechanisms were observed. Of interest is that in isotopically mixed solution the mechanism proposed by Fayer et al. is not observed and the explanation was that energy redistribution over the oligomer led to OH hydrogen bond rather than OD hydrogen bond breaking.⁵²

If one wants to study hydrogen bonds in their most important context, H₂O would seem the system of choice. The Bakker group investigated the vibrational dynamics of water using a femtosecond IR pump-probe laser system.⁵³ Extensive studies of OH stretch in HDO dissolved in D₂O brought evidence for a Stokes shift, i.e. upon excitation a peak was observed at a frequency lower than the incident frequency, with a lifetime of 740 fs. In describing the data quantitatively the hydrogen bond was assumed to be a Brownian oscillator coupled to the excited OH mode, **Figure 2.3**.

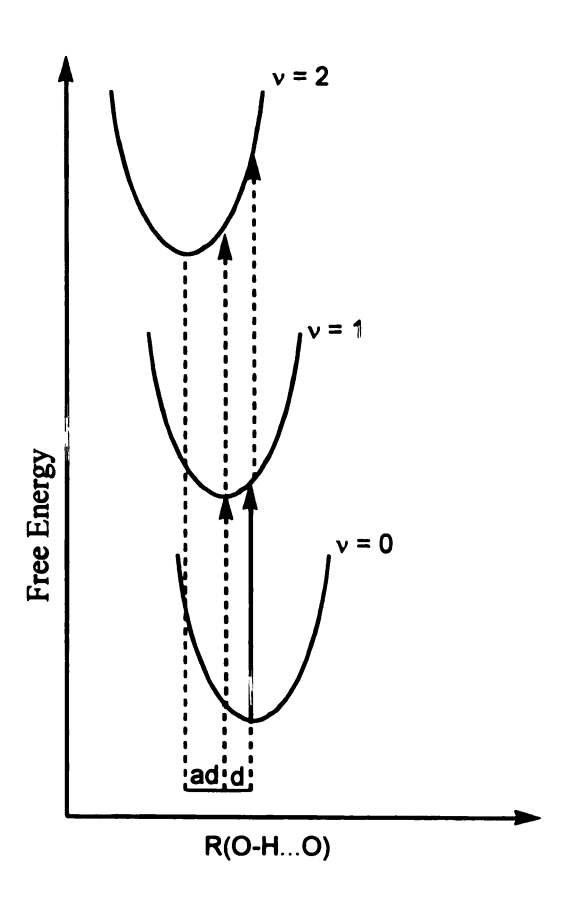


Figure 2.3 Bakker Model for the OH Excited Mode

The Brownian oscillator model is characterized by harmonic potential energy functions for the hydrogen bond mode, which are displaced by a distance d with respect to each other in the ground and excited states of the OH-stretching mode. Also because the OH stretch absorption band had an approximately Gaussian shape and was broad, the authors assumed the hydrogen bond mode to be strongly overdamped, which implies that the wavefunctions associated with the hydrogen bond vibrations are strongly coupled to each other and to other low-frequency liquid modes. The limitations occurred from the not so good description of the spectral relaxation at large delay times. Using the same model Kropman et al. studied the OD stretch of HDO dissolved in H₂O.⁵⁴ The unexpectedly long vibrational lifetime for OD, 1.8 ps, twice as much as the corresponding one for OH, prompted the authors to suggest that despite the fact that the energy gap law would predict the opposite, the number of accessible modes is probably larger for OH.

Using the same laser system, Bakker et al. studied the dynamic behavior of the OH stretch modes in HDO molecules dissolved in a 10 M NaOD solution in D_2O . In the IR spectrum of this solution three OH groups could be distinguished, **Figure 2.4**.

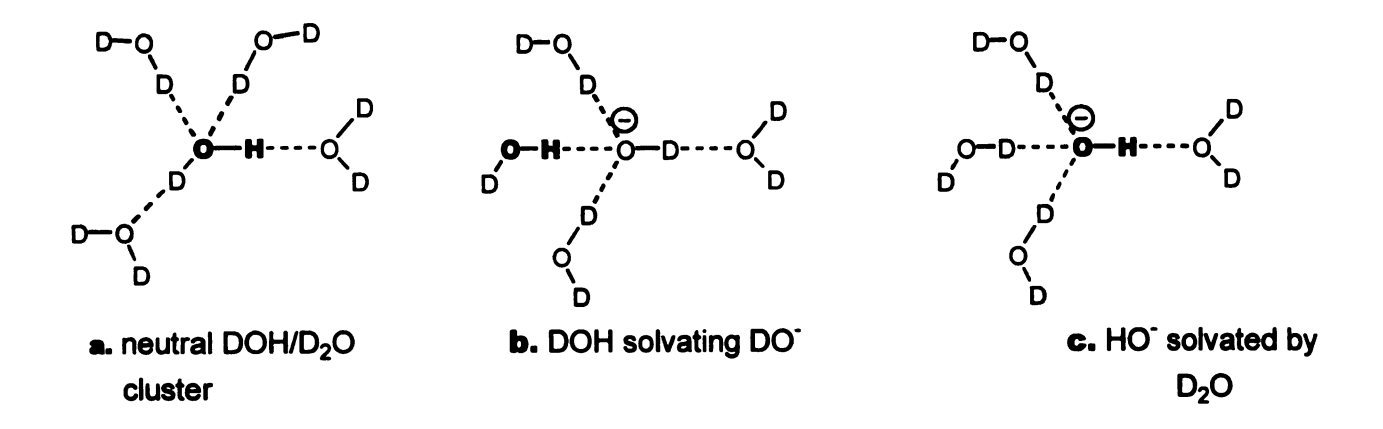


Figure 2.4 10M NaOD Solution in D₂O

In the range 3200-3500 cm⁻¹ are the majority of HDO molecules, which donate hydrogen bonds to other D₂O or HDO molecules, **Figure 2.4**, a. At lower frequencies are HDO molecules that form strong hydrogen bonds with OD, **Figure 2.4**, b. Finally, resonances at 3600 cm⁻¹ were attributed to HO ions, **Figure 2.4**, c. The excitation was applied in all three regions and it was found that persistent spectral holes could be observed in the OH stretch in all three environments, evidence for a more rigid hydrogen bonded network than that of pure liquid water, for which rapid broadening of the hole was observed, with a lifetime of 600 fs.

The behavior upon excitation was rationalized using the brownian oscillator model again. Two components were distinguished. The first component is due to the HDO molecules that are bonded to D₂O as DO-H...OD₂, which have a shorter vibrational lifetime than the HDO molecules in "pure" base free liquid, i.e. no DO or HO present, only HDO

and D_2O , 600 fs compared to 740 fs. The second component corresponds to HDO molecules that are hydrogen bonded to D_2O or OD^- and that participate in proton transfers between HDO and OD^- or deuteron transfers between OD^- and D_2O . The lifetime of vibrational relaxation for this component is ~ 160 fs and was attributed by the authors to the time scale of deuteron hopping. The large difference between the time scales of these two components led to the conclusion that the complexes that generate them are localized in regions of hydrogen bonded network and that they are not interchangeable.

All the work in the Bakker group was rationalized in the light of the brownian oscillator model, which assumes that the motion of the OH is strongly damped due to strong coupling among the hydrogen bonding and liquid modes and thus the dynamics are based on a hydrogen bond length value resulting from interactions with the surrounding liquid. Based on thorough molecular dynamic simulation studies of the HOD/D₂O system, Hynes demonstrated that there is not a simple linear dependence between the frequency of the OH and the length of the hydrogen bond in which that OH is involved and thus interpretation of the experimental data should be based on a range of distances.⁵⁶

Examples of ionic hydrogen bonded systems studied by IR pumpprobe spectroscopy are few and the most representative is the work done is
in the Strauss group on Tutton salts, (NH4)₂[Cu(H₂O)₆](SO₄)₂ and
(NH₄)₂[Co_xNi_{1-x}(H₂O)₆(SO₄)₂, in solid the state at low temperature.^{57, 58}
Upon excitation the hydrogen bonds were broken due to reorientation. The
lifetime of burning holes was estimated to be on minute time scale. The
temperature independence of rate constants prompted the authors to suggest
the occurrence of tunneling.

Another studied ionic system is gas-phase clusters, $Cl(H_2O)_n(CCl_4)_m$, in which excitation led to loss of a H_2O molecule if m=0 and CCl_4 if there is one CCl_4 molecule.⁵⁹

Recently the Bakker group investigated the vibrational dynamics of hydrogen-bonded HCl-diethyl ether complexes. ⁶² Upon excitation of the H-Cl stretching mode, 2500 cm⁻¹, with a 500 fs laser the relaxation was found to take place in two steps. The first step was assigned to the vibrational energy transfer to the hydrogen bond mode with a time constant of 0.9 ± 0.2 ps, causing a shift in the HCl stretching mode absorption. The second step corresponded to the relaxation of the hydrogen bond with a time constant of 3.1 ± 0.5 ps. The authors also reported no evidence for a proton transfer from the HCl to the ether, i.e red shift due to formation of a vibration lower

in energy than the HCl stretch, due probably to the fact that the energy is rapidly transferred to the hydrogen bonding mode.

Complexes in which the hydrogen bond acceptors are different molecules were investigated by Schriver et al. for HI with different partners: water, acetylene, ethylene oxide, dimethyl ether, and acetone in matrix.^{60, 61} Photoirradiation led to cleavage of the hydrogen bonds. Since the laser only accessed frequencies in the range 1600-2500 cm⁻¹, excitation of CH₃ followed by energy redistribution and proton transfer were proposed but no accurate evidence could be found.

1.3. Dihydrogen Bonding

Dihydrogen bonding has been in recent years the subject of extensive experimental and theoretical research. It can be defined as an attractive interaction between the hydrogen of a proton donor, A-H (A=O, N, X) and the σ M-H bond, where M is less electronegative than hydrogen, Figure 3.1.

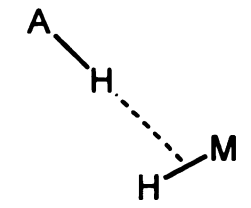


Figure 3.1 Dihydrogen Bonded Complex

With strengths and directionality comparable with those found in traditional hydrogen bonds, dihydrogen bonds play an important role in solid and solution chemistry, controlling structure, reactivity and selectivity.

Possible applications include stereochemical control, catalysis, crystal engineering and material chemistry and numerous reviews have summarized the achievements⁶³ with the most recent one from the Epstein group.⁶⁴

1.3.1 Dihydrogen Bonding in Main Group Hydrides

The ability of boron hydrides to serve as proton acceptors in hydrogen bonds was observed by M. P. Brown et al. in 1968. Variable temperature infrared spectroscopy studies of LBH₃ (L=Me₃N, Et₃N, Py, Et₃P) and Me₃NBH₂X (X=Cl, Br, I) in the presence of proton donors such as methanol,

propanol, and p-fluorophenol in CCl₄ led to values for the association energy in the range 1.7-3.5 kcal/mol. Based on the perturbation of N-H stretch with temperature and concentration, they also suggested a NH...H₃B interaction in Me₂NHBH₃ and (RNHBH₂)₃ (R=Pr, Bu).⁶⁵⁻⁶⁷

Epstein et al. studied NEt₃BH₃, P(OEt)₃BH₃, and Bu₄NBH₄ in the presence of different proton donors by solution NMR and IR spectroscopy and they noted the occurrence of O-H...H-B interactions with properties similar to those found in classical hydrogen bonds.^{68,69} The association energies increased with the proton donors' acidities, falling in the range 1.1-3.7 and 2.3-6.5 kcal/mol, for neutral and ionic hydrogen bonds, respectively.⁷⁰

In the Jackson group the X-ray and neutron crystal structures of $NaBH_4\cdot H_2O$ and $NaBD_4\cdot D_2O$ were determined and O-H...H-B dihydrogen bonding was observed with three H...H close contacts, 1.79, 1.86, and 1.94 Å. Also the O-H vectors point toward the middle of the B-H bonds, suggesting association with the σ -bond electrons, rather than B or H atoms.⁷¹

Crabtree et al. searched the Cambridge Structural Database (CSD) for close intermolecular B-H...H-N contacts of which 26 were found in the range 1.7-2.6 Å. These compounds have a bent geometry with NH...H-B angles in the range of 95-120°. The authors suggested that this structure is

due to the presence of negative charges on both B and H atoms so that the bending allows close proximity between protonic NH and B with maximum attractive electrostatic interaction. Theoretical study on a NH₃BH₃ dimer, at the B3LYP/PCI80 level of theory, confirmed two H...H interactions, at 1.82 Å distance, and 98.8°NH...H-B angle, falling in the range found by the CSD search. The association energy was predicted to be 6.1 kcal/mol per dihydrogen bond, which could be responsible for the difference in melting points between the isoelectronic borane (+104 °C) and ethane (-181 °C).⁷²

In a subsequent paper on NH₃BH₃, the geometry found by Cramer and Gladfelter, at the MP2/cc-pVDZ level, has bifurcated dihydrogen bonds, with H...H distance of 1.99 Å, NH...H-B angle of 88.6°, and association energy of 15.1 kcal/mol. The X-ray structure of (NH₃BH₃)₂ dimer reported by Crabtree et al. shows three intermolecular H...H interactions, the shortest at 2.02 Å, and NH...H-B angle of 106° . The N-H vectors point toward the middle of the B-H bonds , suggesting again that the interaction is between the proton and the σ -bond electrons. The N-H...H-B dihydrogen bonding interaction was characterized was also characterized in compounds other than aminoborane by crystallographic methods and by ab initio calculations. The N-H-S dihydrogen bonding

The hydrides of Ga and Al, elements in the same group as B, are also capable of forming dihydrogen bonded complexes. Intramolecular N-H...H-Al close contact was observed in an alane piperidine adduct by Raston et al with a H...H distance of 2.31 Å, Figure 3.2, in an eclipsed conformation.⁸⁰ The authors noted that the structure undergoes H₂ loss to form an amidoalane.

Figure 3.2 Alane Piperidine Adduct

Ab initio studies by Cramer and Gladfelter for (NH₃AlH₃)₂ dimer, at the MP2/cc-pVDZ level, showed two intermolecular H...H contacts at 1.78 Å, and an interaction energy of 6 kcal/mol per dihydrogen bond.⁸¹ Cyclotrialumazane, [(NH₂AlH₂)₃]₂ dimer has been found to have a C_{3v} symmetry with 6 H...H contacts and dimerization enthalpy of -9.9 kcal/mol, Figure 3.3.⁸³

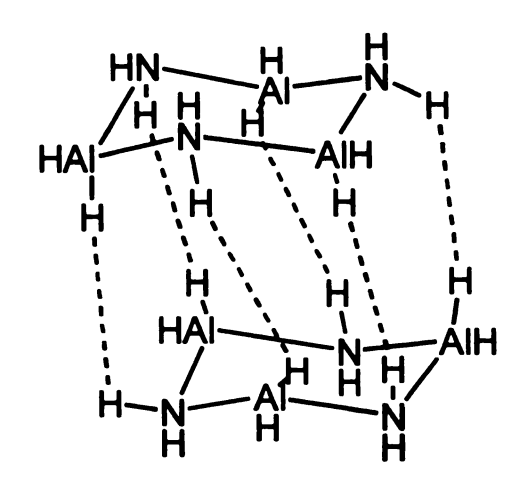


Figure 3.3 Cyclotrialumazane

The ability of Ga to participate in dihydrogen bonds was confirmed by the neutron diffraction crystal structure of cyclotrigallazane.⁸¹ Theoretically the strength of the dihydrogen bond was predicted to be 3 and 5 kcal/mol/bond for [(NH₂GaH₂)₃]₂ and (NH₃GaH₃)₂ respectively.

Extensive ab initio theoretical work investigated the occurrence of dihydrogen bonds in complexes involving other main groups hydrides. 82-89

Based on thorough theoretical investigation of complexes between group I,

II, and IV hydrides with HF, Grabowski demonstrated correlation between

H...H distances and dihydrogen bonding energies. 88, 89

1.3.2 Dihydrogen Bonding involving Transition Metal Hydrides

In 1990, Koetzle et al. reported the neutron diffraction crystal structure of [Ir(PMe₃)₄(H)(OH)]⁺ in which a H...H contact of 2.4 Å and an Ir-O-H angle of 104° suggested an attractive interaction, **Figure 3.5**.⁹⁰

$$L = PMe_{3}$$

$$H \longrightarrow H$$

$$L = PEt_{2}H$$

Figure 3.5 [Ir(PMe₃)₄(H)(OH)]⁺ and [Fe(H)₂(H₂)(PEt₂Ph)₄] Complexes
A shorter H...H distance, 1.862 Å, was observed in [Fe(H)₂(H₂)(PEt₂Ph)₄]
and prompted the authors to suggest an intramolecular hydrogen bond,
Figure 3.5.⁹¹

The Morris and Crabtree groups independently discovered the first example of intramolecular dihydrogen bonding in Ir hydride complexes.

Crabtree 92 showed evidence for Ir-H...H-O interaction facilitated by tautomerization of the ligand into an iminol, 1.

X=PPh₃

1

The calculated H...H distance was 1.8 Å. The coupling between the Ir-H and O-H hydrogens, 3 Hz, led to the conclusion that the interaction had a covalent character. A higher coupling, 5.5-5.6 Hz, was found when the ligand was pyridine 93 (Y=H, Cl, Br, I), in which the H...H distance was calculated to be 1.7 Å for Y = Cl, 2.

In order to estimate the dihydrogen bond strength, Crabtree measured the rotation barrier for the NH₂ group in a series of 2-aminopyridine complexes⁹³ (3), which represents the sum of the intrinsic rotation barrier and dihydrogen bond. The strongest dihydrogen bond was found to be 5.0 kcal/mol when Y=H. Also the Y ligand weakens the interaction in the order F>Cl>Br>I>CN>CO>H which correlates with electronegativity decrease. Thus, as the hydride becomes more negative, the NH...HIr interaction becomes stronger.

32

Ir-H...H-N interactions were demonstrated by the Morris group⁹⁴ via X-ray diffraction and solution NMR for an Ir hydride complex, The H...H close contact distances, calculated from relaxation times, were 1.75Å. Theoretical calculations by Hoffmann et al. on a model compound, L=PH₃, confirmed the interaction and concluded that its nature is mostly electrostatic.⁸²

The interaction was turned off by the presence of a competing hydrogen bonding solvent, tetrahydrofuran.⁹⁴ Morris et al. also showed evidence for

occurrence of bifurcated dihydrogen bonds with estimated distances of 1.8 and 1.86 Å (Figure 3.6). 95

Figure 3.6 Bifurcated Dihydrogen Bonds in Ir Hydride Complexes

The first example of intermolecular dihydrogen bonding involving a transition metal hydride was reported by Crabtree et al. for a Re polyhydride, 5, based on compound's X-Ray structure.⁹⁶

The geometry and energetic characteristics corresponded to a dihydrogen bond and were confirmed by theoretical calculations on model compound [ReH₅(PH₃)₃]·NH₃.^{97, 98} The intermolecular A-H...H-Re were reported in complexes between imidazole, 2,4,6-Me₃C₆H₅OH, 2-tBu-6-MeC₆H₃OH, pyrrole, Ph-NH-Ph, Ph-NH-Bu, Ph-NH-Me and ReH₅(PPh₃)₂ with interaction energies in the range 3.0-5.8 kcal/mol.⁹⁹ Substitution of ReH₅(PPh₃)₂ with WH₄(PMePh₂)4 allowed Crabtree to demonstrate the ability of W to participate in this type of interaction. Re-H...H-N interactions were studied in solution by Crabtree using UV-VIS spectroscopy.¹⁰⁰

Shubina et al. explored the dihydrogen bonding in solution between tungsten hydrides and alcohols (Figure 3.12).

L = PMe₃, PEt₃, P(i-PrO)₃, PPh₃ R = Ph, CH(CF₃)₂, C(CF₃)₃

Figure 3.7 Dihydrogen Bonds in W Hydrides

Using IR and NMR spectroscopy they excluded the hydrogen bonding to CO and NO groups and demonstrated occurrence of the O-H...W-H interactions. The association energies fall in the range of expected dihydrogen bonds and correlate to the acidity of the proton donors. They proposed a linear

OH...H-W orientation in contrast to the previously found bent geometry of dihydrogen bonds.¹⁰¹

The same group reported the occurrence of intermolecular O-H...H-Re in solution and theoretically. ^{102, 103} The ability of the solvent to interact via π...H-O and the bulk of the ligand appear to influence the dihydrogen bonding. The Scheiner group reported elegant theoretical studies on Mo and W hydrides complexes, 6, and confirmed the correlation between the dihydrogen bond strength and the acidity of the proton donor or the donating ability of the cis ligand. ¹⁰⁴

When the proton donor is H_3O^+ , proton transfer takes place with the formation of an η^2 - H_2 dihydrogen complex. All the optimized complexes have strongly bent geometry.

36

1.4. Proton Transfer in Dihydrogen Bonded Systems

Dihydrogen bonds have been proven to have strength and directionality comparable with conventional hydrogen bonds. What makes them unique is their ability to undergo proton transfer and H_2 loss with or without participation of an η^2 - H_2 intermediate (Scheme 4.1).

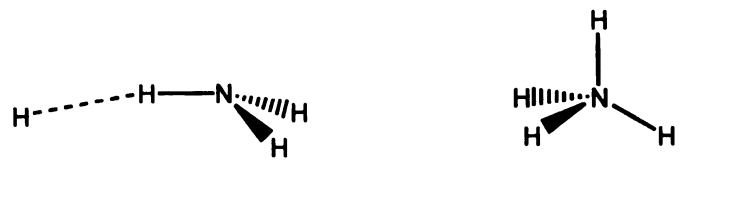
Scheme 4.1

The simplest systems to be studied theoretically are the ones in which the proton acceptor is H, the hydride itself. Ab initio calculations by Cremer and Kraka, at the MP2/6-31+G* level on NH₄ and H₃O predicted association energies of 9.1 and 18.7 kcal/mol, respectively, in complexes with geometries consistent with dihydrogen bonded complexes. The proton transfer barriers were 10.4 and 7.0 kcal/mol, respectively. In the case of NH₄ a minimum with tetrahedral geometry was also optimized, higher in energy than the dihydrogen bonded structure by 1.3 kcal/mol. This entity should be envisioned as a Rydberg system.

The Gordon group investigated the NH₄ ion at the MP2/6-311++G** level and reported geometries similar with the ones found by Cremer and

Kraka. 106 However the energy of the tetrahedral structure was estimated to be 10.0 kcal/mol higher (Figure 4.1).

Figure 4.1 NH₄ Structures



dihydrogen bonded complex

tetrahedral structure

Intrinsic reaction coordinate calculations showed that this structure is not connected to the transition state or the products of the proton transfer reaction. The authors performed a dynamic reaction coordinate calculation on the tetrahedral structure and they noted that proton transfer took place upon excitation with 32.5 kcal/mol. It should be noted that the tetrahedral structure is higher in energy than the transition state for proton transfer.

Since its first mass spectrometric observation in 1982 by Paulson and Henchman, 107 the H_3O^- ion has received considerable attention. In a mass spectrometric study by Miller et al., rate constants for formation of the H_3O^- anion and its reaction with a large number of reagents have been measured. The association energy was found to be 14.4 ± 1.0 kcal/mol and dissociation of H_3O^- into HO^- and H_2 required 4.5 ± 1.0 kcal/mol. 108 Investigation of the $HO + H_2 \rightarrow H_2O + H$ reaction via photodetachment spectroscopy of H_3O^- , paralleled by ab initio calculations, led to values for

the dihydrogen bond and barrier for proton transfer in good agreement with the previously calculated ones, 18.7 and 3.80 kcal/mol, respectively. 109

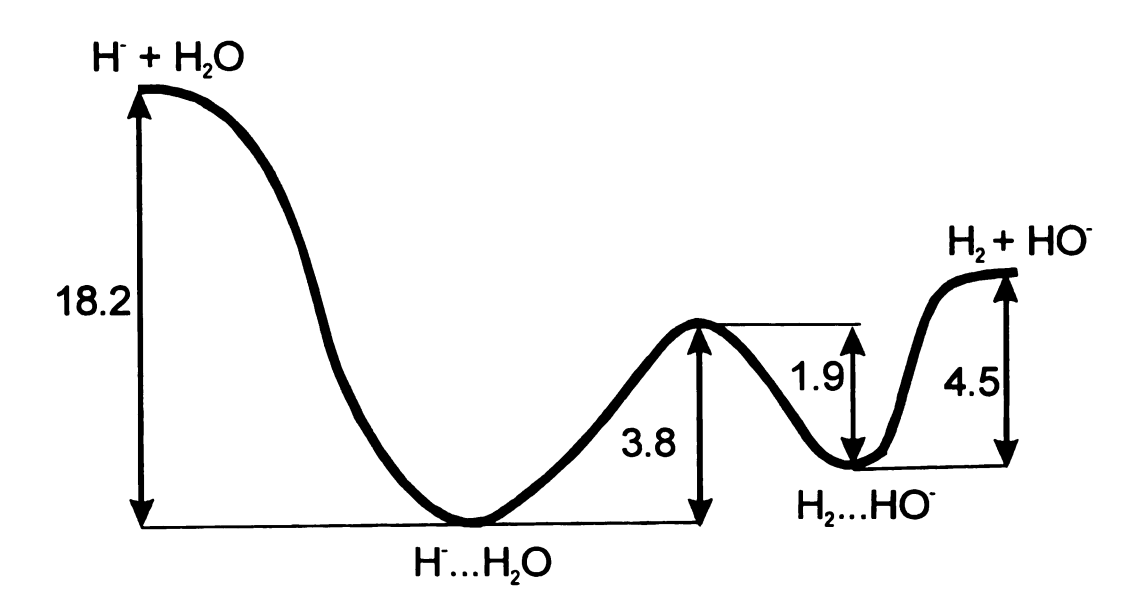


Figure 4.2 Proton Transfer in the H₃O Complex

Dihydrogen bonding could influence the reactivity of the bonds involved in the interaction. Crabtree et al. reported that the hydrogens involved in dihydrogen bonding, H_a and H_b, in an Ir hydride complex, could undergo scrambling, whereas the non-interacting hydrogen, H_c, was exchanged much more slowly with either H_a or H_b, (Scheme 4.2).¹¹⁰

 $L = PPh_3$ R = Me, n-Bu, p-TOLYL, Ph, p-FC₆H₄, 3,4-C₆H₃F₂

The ΔG^{\neq} was found to be 16 kcal/mol (R = Ph) and gets smaller as the R group becomes more electron withdrawing which is consistent with a mechanism involving proton transfer from OH to give an η^2 – H_2 complex. Rotation of H_2 and proton back transfer completes the process. When the solvent was benzonitrile, the H_2 ligand was displaced by PhCN in a rate-determining step. Heating the dihydrogen bonded complex at 80 °C in a sealed tube led to H_2 loss with formation of an Ir-O σ bond. The process could be reversed at 20 °C in CH_2Cl_2 with exposure to H_2 (Scheme 4.3).

$$H_{c}$$
 H_{c}
 H_{b}
 H_{c}
 H_{b}
 H_{c}
 H_{b}
 H_{c}
 H_{c

An analogous hydrogen exchange process was observed for the aminopyridine complexes (Scheme 4.4).¹¹²

The reaction is first order with respect to the complex with a large negative value for $\Delta S^{\neq} = -32$ e.u, pointing in the direction of a highly organized transition state.

Chaudret et al. documented the dynamic equilibrium between a dihydrogen bonded complex and an η^2 -H₂ complex, using NMR spectroscopy. ¹¹¹ In benzene or toluene, the RuH₂(dppm)₂•PhOH complex exists as a mixture of dihydrogen bonded trans and cis isomers, but only the trans isomer is involved in a dynamic equilibrium with the dihydrogen bonded complex, which is 17 kcal/mol more stable. The driving force for the reversibility of the process was suggested to be the strength of the dihydrogen bond. As expected in the presence of a more acidic proton donor, such as (CF₃)₂CH-OH, the η^2 -H₂ complex undergoes H₂ loss (Scheme 4.5).

Theoretical work¹¹² done by Scheiner et al. on

HOH...H₂Ru(PH₂CH₂PH₂)₂ model complex estimated a barrier for proton transfer of 10 kcal/mol and a reaction enthalpy of 10.7 kcal/mol. However when HF was used the only minimum localized on the potential energy

surface (PES) was the η^2 -H₂ complex, which was found to be 23.8 kcal/mol more stable than the free species.

The Epstein group investigated proton transfer by solution IR and NMR spectroscopy in dihydrogen bonded complexes between (triphos)Re(CO)₂H and different proton donors: phenol, tetrafluoroboric acid, chloroacetic acid, hexafluoro-2-propanol, and perfluoro-2-methyl-2-propanol at 200-260 K. The η^2 -H₂ complexes were more stable than the corresponding dihydrogen bonded ones and increases in temperature induced H₂ loss with the formation of the Re-O σ bond (Scheme 4.6).

Scheme 4.6

For the $H_2Re(CO)(NO)(PMe_3)_2 \bullet CF_3COOH$, and $W(H)(CO)_2(NO)(PMe_3)_2 \bullet$ (CF₃)₂CHOH systems the η^2 -H₂ complex was unstable. In the case of HRu(Cp)(CO)(PCy₃) with (CF₃)₃COH the η²-H₂ complex is stabilized by ion pair formation. The barrier for proton transfer in the latest complex was found to be 15 kcal/mol.¹¹⁴ The interaction between (Cp)Re(H)(NO)(CO) or (Cp)Ru(H)(CO)(PH₃) hydrides and proton donors of different strength, such as H₃O⁺, H₂O, and CF₃OH, was studied by Scheiner et al in order to model the reaction investigated by Epstein.¹¹⁵ They found that the dihydrogen bonded complex strength and the proton transfer barrier are strongly influenced by the proton donor ability of the acid.

Chaudret and coworkers documented the proton transfer in a dihydrogen bonded complex between a Ru hydride and (CF₃)₂CHOH when the solvent is CDCl₂F/CDF₃ (2:1) at low temperature. This Freon mixture was selected to increase the solution's dielectric constant at low temperature. The proton transfer took place only at a temperature low enough to induce the required change in the dielectric constant. The same behavior could be observed when the solvent was CD₂Cl₂ (dielectric constant of CD₂Cl₂ increases from 9 at room temperature to 17 at 170 K).

N-H...H-Ru dihydrogen bonds are able to undergo proton transfer as observed by Lau et al. 117 (Scheme 4.7). H/D exchange for both hydridic and protonic hydrogens in D₂O, proved the equilibrium between the dihydrogen

bonded and η^2 -H₂ complexes. The hydrogenolysis of the Ru-N bond could be done at 60 °C under 60 atm of H₂ pressure.

Scheme 4.7

n = 2, 3

The covalent system was found to catalyze the reduction of CO_2 to HCOOH, although in small yields. The proposed mechanism involves a heterolytic splitting of the H_2 ligand (Scheme 4.8).¹¹⁷

The detection of the dihydrogen bonded complex by NMR suggested that the CO₂ insertion is the rate determining step. Subsequent theoretical calculations supported this conclusion. ¹¹⁸

Noyori et al. reported that theoretical studies on hydrogen transfer between alcohols and carbonyl compounds catalyzed by Ru(II) complexes containing NH or NH₂ ligands predicted the involvement of NH/NH₂ group in the reaction (**Scheme 4.9**). The implications of the intramolecular N-H...H-Ru dihydrogen bond in the catalyst complex were not investigated.

The Morris group used a diamine, NH₂C(CH₃)₂C(CH₃)₂NH₂ (tmen), and provided experimental evidence for the catalytic cycle predicted by Noyori. Moreover they concluded that the N-H...H-Ru is responsible for enantioselectivity observed in these reactions.¹²⁰

Chaudret et al. reported hydrogen exchange in a related complex, 7, using NMR spectroscopy, and the activation barrier for the process was found to be 11 kcal/mol.

However theoretical calculations¹²¹ predicted that the exchange mechanism does not involve proton transfer within the dihydrogen bond (**Scheme 4.10**). Instead the evidence pointed to direct proton transfer to the metal itself.

Scheme 4.10

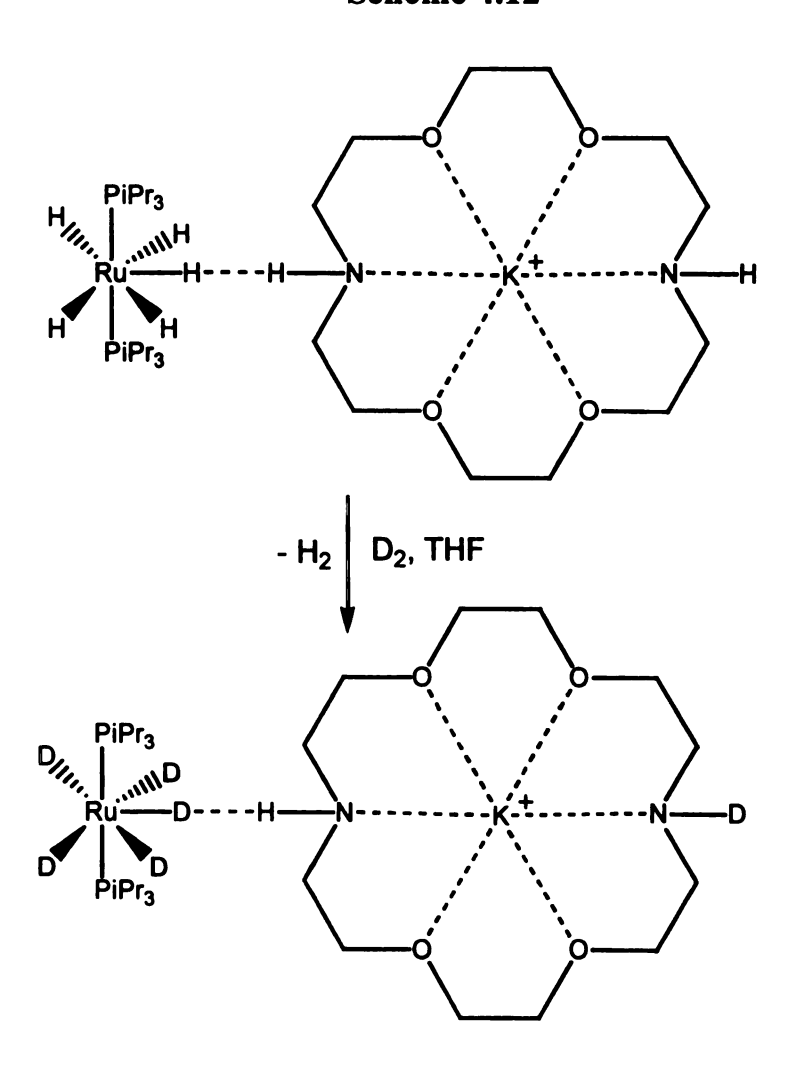
A three-center intramolecular dihydrogen bonded complex and its dynamics were reported by Jalon et al. ¹²² The fast exchange between the hydridic and protonic hydrogens was believed to occur via an η^2 -H₂ intermediate (Scheme 4.11) with a barrier of 13.6 kcal/mol as determined via NMR spectroscopy.

When a solution of the dihydrogen bonded system in CD_3OD was exposed to H_2 atmosphere at room temperature and 1 atm, more than 90% of the H_2 was exchanged for D_2 in about half an hour.

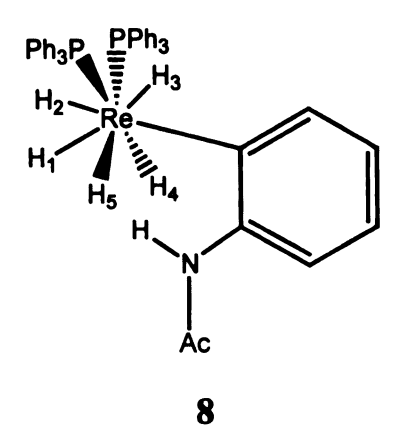
The Morris group reported a similar exchange in a ruthenium polyhydride complex, K[(1,10-diaza-18-crown-6)][RuH₅(PiPr₃)₂] (**Scheme 4.12**). Upon exposure to D₂ at room temperature and 1 atm for 5 min, the intensities of the protonic and hydridic hydrogens were depleted by 100% and 90%, respectively. When 18-crown-6 ether was used only 13 %

depletion was observed after 10 days. Also replacement of Ru hydride by the less basic Os hydride induced a slower exchange. Control experiment excluded RuH₂(H₂)(PiPr₃)₂ as an intermediate.

Scheme 4.12



Intramolecular N-H...H-Re were considered to be responsible for hydride fluxionality in $ReH_5(PPh_3)_2L$, (L = N-acetyl-2-aminopyridine), 8.



The activation energy for rotation, involving H₁, H₄, and H₅, is 0.7 kcal/mol smaller with the NHAc group in ortho than in para suggesting that the transition state is stabilized by dihydrogen bonding.¹²⁴ However theoretical calculations showed that the two hydrogens involved in the dihydrogen bonding are forced to be 1.49 Å apart at the transition state.¹²⁵

Stereoselectivity and reactivity can be influenced by dihydrogen bonding. By stabilizing one particular transition state among many others, they can control the product distribution and/or the stereochemical outcome. This concept was demonstrated by Crabtree et al. in the selective imination of an Ir aldehyde complex with ortho- versus para- hydroxyaniline(Scheme 4.13).

When an equimolecular mixture of reactants, 2-aminophenol, 4-aminophenol, and Ir aldehyde complex, was used a 4.2:1 products ratio was obtained which corresponded to a k1/k2 ratio of 6. The authors concluded that the driving force was the dihydrogen bonding which stabilized the product and the corresponding transition state. The two products do not interconvert indicating that the product distribution is due to kinetic control.

The dihydrogen bonding was estimated to be stabilizing by 4.5 kcal/mol while $\Delta\Delta G^{\neq}$ between the two reactions was found to be 1.1 kcal/mol. The difference was suggested to come from the unfavorable ring conformation required for dihydrogen bonding at the transition state.

Aime et al. showed that dihydrogen bonding could control the regiochemistry of ligand attachment in transition metal complexes.¹²⁷ When an unsaturated Os complex was reacted with EtNH₂ or Et₂NH only the syn product was observed (**Scheme 4.14**). The intramolecular bond would not be possible in the anti isomer. When Et₃N was used no reaction occurred.

Scheme 4.14

$$(OC)_3Os \xrightarrow{\qquad \qquad \qquad } Os(CO)_4 \xrightarrow{\qquad \qquad } Os(CO)_3 \xrightarrow{\qquad \qquad } Os(CO)_4 \xrightarrow{\qquad \qquad } Os(CO)_3$$

 $L = Et_2NH, EtNH_2$

R = Et, H

Treatment with NH₃ followed by acetaldehyde or acetone in CHCl₃ led to the exclusive formation of the syn product with an intramolecular dihydrogen bond (Scheme 4.15).

$$(OC)_{3}Os \xrightarrow{Os(CO)_{4}} Os(CO)_{3} \xrightarrow{1. NH_{3}} Os(CO)_{3} \xrightarrow{Os(CO)_{4}} Os(CO)_{3} \xrightarrow{Os(CO)_{3}} Os(CO)_{3}$$

When CHCl₃ was replaced with a more polar solvent capable of hydrogen bonding, such as methanol, the N-H...H-Os was disrupted. NMR spectroscopy studies showed that the outcome in this system is dictated by thermodynamic control.^{128, 129}

In the Jackson group, it was proved that O-H...H-B dihydrogen bonds could accelerate and direct the borohydride reduction of ketones to alcohols. The reductions of 2-hydroxycyclobutanone or 2-hydroxycyclopentanone with NBu₄BH₄ in non hydrogen bonding solvents, such as CH₂Cl₂ and ortho-C₆H₄Cl₂, were accelerated by 150 times relative to the reductions of corresponding unsubstituted cycloalkanones. At the time the findings appeared to indicate high stereoselectivity but as will be discussed in chapter 4 more recent results suggest a less clear-cut picture.

2. Dynamic Studies for Proton Transfer in Dihydrogen-bonded Complexes involving AlH₄

In principle, deposition of sufficient vibrational energy into a chemical bond's stretching mode should induce its rupture, resulting in an Infrared-pumped reaction (IRPR). At the same time the vibrational relaxation is very fast, usually beating any process that actually effects chemical change. The challenge to those who would design IRPRs is thus clear: the reaction time must be competitive with the relaxation time of the vibrational mode in question; the energy deposited must of course be adequate to surmount the activation barrier (including thermal and tunneling contributions) for the process; and the overall reaction should be irreversible or at least exothermic (i.e. the back reaction should have a high barrier). We have used ab initio methods to explore a class of candidate reaction systems that appear to meet these requirements.

Dihydrogen bonded complexes A-H...H-M (A = O, N, Halogen; M = metal) offer several attractive features which should make them good substrates for reaction via single-photon infrared excitation. As in any A-H...B hydrogen bond, the A-H stretch vibrations are typically isolated at the high energy end of the IR spectrum, in the 3-4000 cm⁻¹ range (i.e. ca.

8-12 kcal/mol), and are preorganized to align the corresponding normal mode motions with the reaction coordinate for proton transfer. Also, a range of potential energy surface behaviors is possible; depending on the components' relative acid/base strengths, the complex dissociation energies become larger while the barrier to proton transfer decreases. Unique to the hydridic-to-protonic class of hydrogen bonds, proton transfer from A-H to H-M triggers irreversible loss of H₂ and new A-M bond formation. The most active atoms in this process are both hydrogens (proton and hydride), light particles capable of quantum mechanical tunneling, which may allow them to move on a timescale competitive with vibrational relaxation.

In the Jackson group, R. Custelcean has explored this mode of reaction in a number of solid state complex materials using ordinary thermal excitation. Of particular relevance is the solid state kinetic study of LiBH₄·TEA (TEA = triethanolamine; IUPAC name tris(2-hydroxyethyl)amine) in which a value of \approx 20 kcal/mol was deduced for the rate determining initial proton transfer. This value is quite similar to the activation energy value found by Mesmer and Jolly for the solution hydrolysis of BH₄⁻ in H₂O. 132

As noted above, a dihydrogen bonded complex may offer an opportunity for an IRPR. The H...H association preorganizes the system,

and therefore this reaction may be able to proceed rapidly enough to outpace vibrational energy redistribution, a process that normally occurs much faster than chemical reactions.

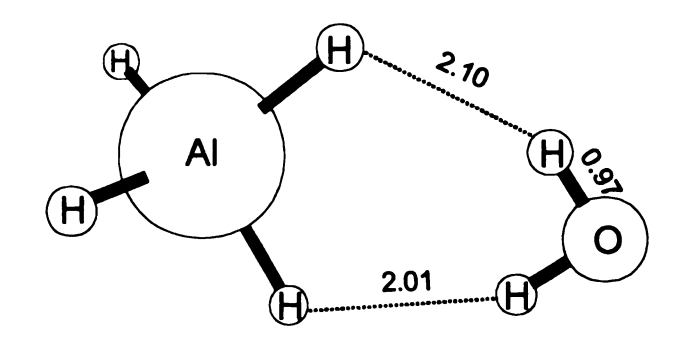
Because Al belongs to the same group as B and Ga and aluminum hydrides are widely used reducing reagents, we have considered that it would be of interest to study AlH₄ as a candidate for M-H and to model the proton transfer reaction for H...H complexes involving AlH₄. Three A-H partners have been considered: H-OH, H-F, and H-Cl.

2.1 Reactants, Transition States and Products

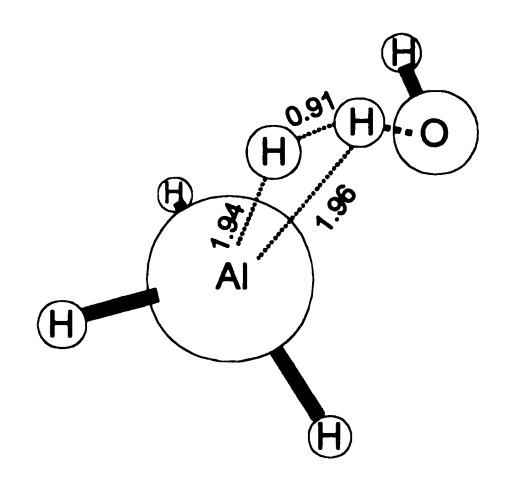
The common features of a dihydrogen bonded complex, A-H...H-M, as noted in chapter 1.2, are close H...H contacts distances, smaller than the sum of the Van der Waals radii of the atoms involved in the interaction, bent geometry, elongation of the A-H bond, and association energies comparable with those corresponding to traditional hydrogen bonded complexes.

In the calculated simulations, at the MP2/6-311++G** level, all the proton donors considered, H₂O, HF and HCl, formed dihydrogen bonded complexes with AlH₄⁻, as defined by a H...H contact distance <2.4 Å, the sum of the Van der Waals radii.

Figure 5.1 [AlH₄...H₂O] Complex Structures: Reactant, Transition State, and Products



Reactant



Transition State

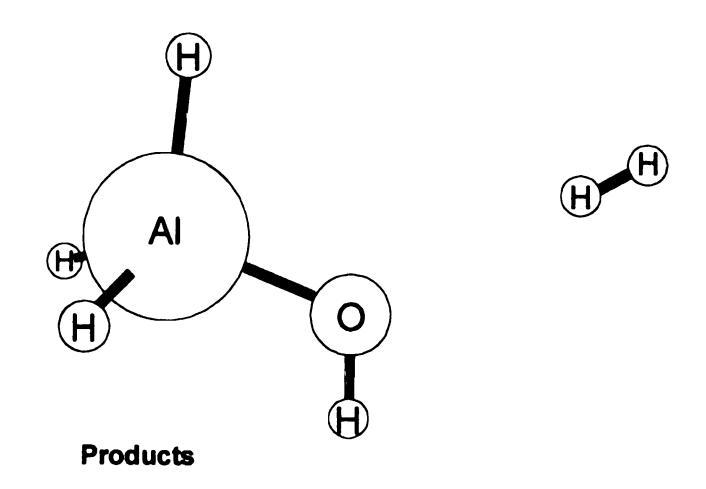
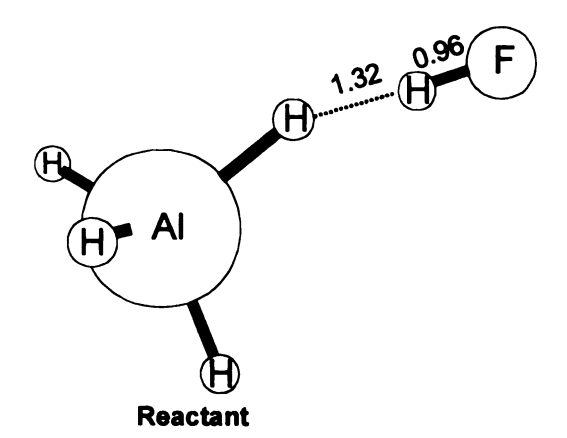
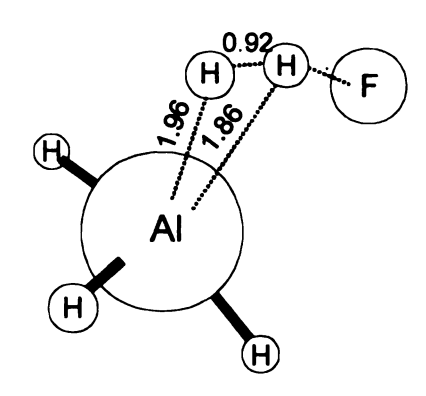
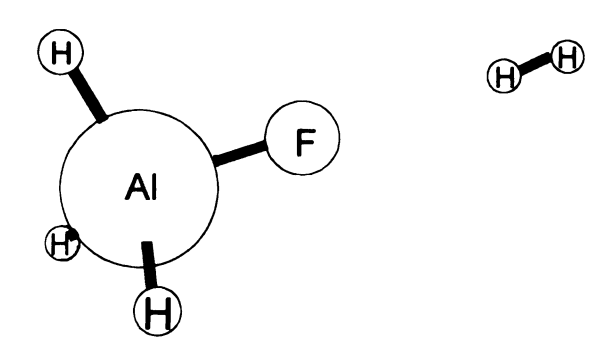


Figure 5.2 [AlH4...HF] Complex Structures: Reactant, Transition State, and Products



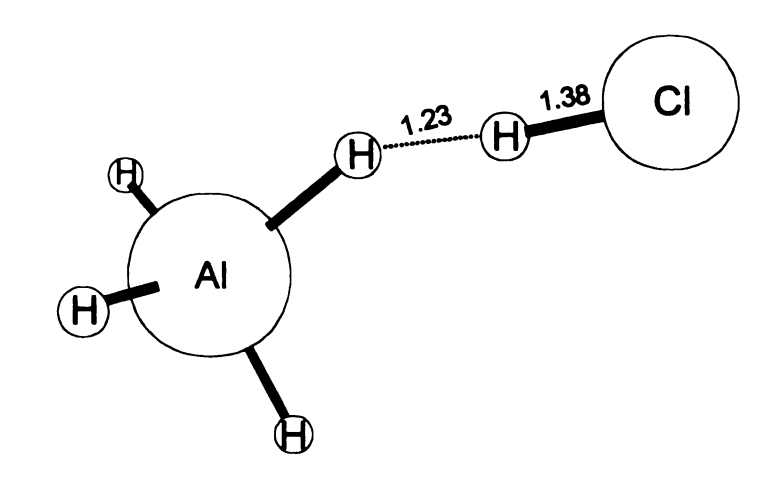


Transition State

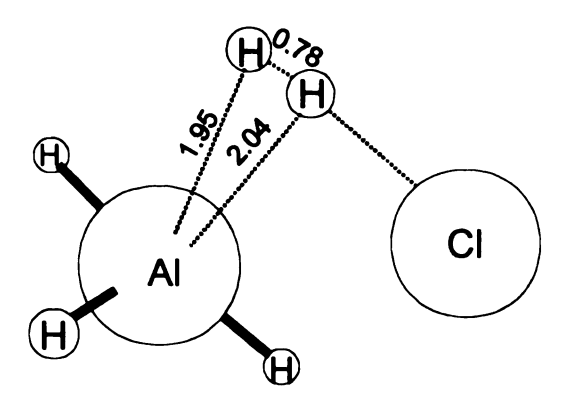


Products

Figure 5.3 [AlH₄...HCl] Complex Structures: Reactant, Transition State, and Products

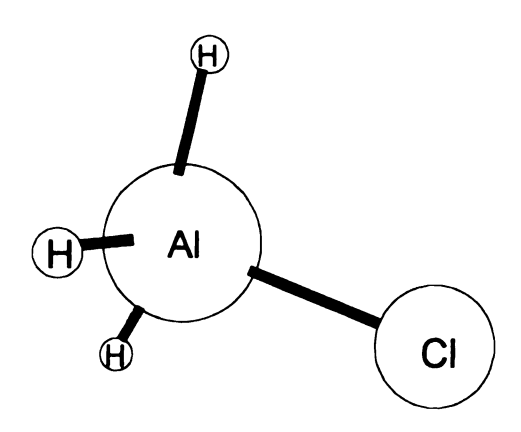


Reactant



Transition State





Products

The complexes geometry is slightly bent, with the H(A)-H(Al)-Al (A=F, Cl) angles falling in the range 140-150°. In the [AlH₄...H₂O] complex, **Figure 5.1**, both protons from H₂O form dihydrogen bonds and thus the small values for the H(O)-H(Al)-Al angle, 109.5 and 110.1°. As expected the elongation of A-H (A=OH, F, Cl) increases with the acidity of the proton donor and the H...H close contact distances vary in the same direction, the smallest value corresponding to the [AlH₄...HCl] complex.

A weaker elongation was observed for the H-Al bond involved in dihydrogen bonding together with shrinkage of the other H-Al bonds. The elongation and the bending in geometry are consistent with known experimental structures, and are interpreted as an indication that the interaction is between the proton and the σ -bonding electrons of the Al-H bond. **Table 5.1** summarizes the relevant geometrical findings.

Table 5.1 Dihydrogen Bonded Complexes: Geometries

A	H-Aª		H(A)-H(Al) ^a	H(A)-H(Al)-Al ^b
	Free	Complex	Distance	Angle
0	0.960	0.967	2.009; 2.009	109.5; 110.1
F	0.917	0.956	1.371	143.0
Cl	1.273	1.381	1.226	149.4

a. in Å, b. in degrees

The association energy – calculated as difference between the complex's energy and the sum of the free partners energies, AlH₄ and HA, and corrected by the zero point vibrational energy (ZPVE) – has been predicted to be 10.14 kcal/mol for the [AlH₄...H₂O] complex and corresponds to 5.07 kcal/mol/dihydrogen bond. Interestingly, the strength of the dihydrogen bond does not increase with the acidity of the proton donor, 15.45 and 13.87 kcal/mol for [AlH₄...HF] and [AlH₄...HCl] respectively. The calculations have also reproduced the experimentally observed shift of the A-H stretch to lower frequency upon association, a feature common to most hydrogen bonded complexes (see **Table 5.2**).

Table 5.2 Energetics of Proton Transfer Reaction for Dihydrogen Bonded Complexes

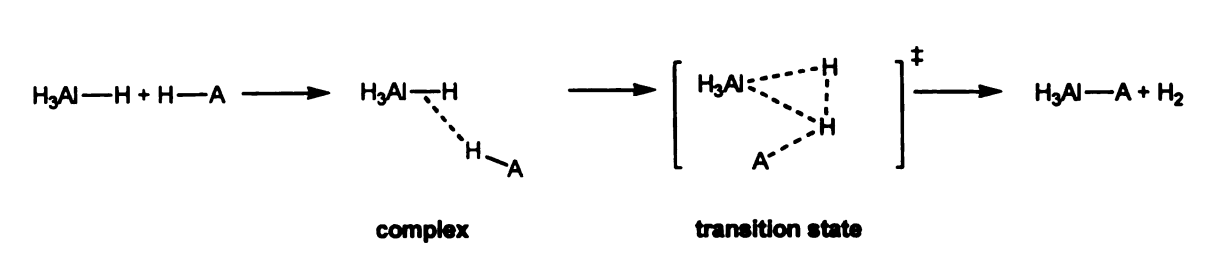
A	$\Delta \mathbf{E_{complex}}^{\mathbf{a}}$	ΔE,ª	$\Delta \mathbf{E_{rxn}}^{\mathbf{a}}$	H-A Vibration ^b	
	•			Free	Complex
ОН	10.2	16.0	27.5	3884; 4003	3797; 3847
F	15.5	19.0	20.9	3325	2200
Cl	13.9	6.7	31.4	3087	1978

a. in kcal/mol, b. in cm⁻¹

The potential energy surface (PES) for each proton transfer/hydrogen loss reaction was initially explored via a relaxed scan in which the H...H distance was stepped from the complex value to the distance in molecular H₂

with reoptimization of all other geometrical parameters at each selected H...H distance. In each case, only one maximum was found, suggesting that the reaction occurs via a concerted process, **Scheme 5.1**.

Scheme 5.1



The structure with the highest energy was optimized to a transition state and a vibrational analysis was performed in order to check the nature of the saddle point. All the transition states have both the proton and the hydride in close proximity to the Al at distances in the range of 2.0 Å (see Figures 5.1, 5.2, 5.3).

Previous calculations¹³³ at the CSD(T)/TZ2P(f,d) level done by Schleyer et al. concluded that AlH₅ is a weak complex between alane (AlH₃) and a slightly elongated H₂ molecule with an association energy of 1.7 kcal/mol at 0 K. At room temperature AlH₅ was found to be unstable toward dissociation by 3.1 kcal/mol; evidently formation of the weak tricentric bond barely perturbs the 104 kcal/mol H-H bond strength, consistent with the high (22 kcal/mol) barrier calculated for scrambling between H₂ and AlH₃ hydrogens.

As expected, the barrier for proton transfer drops dramatically with decreasing H...H distance in the energy minimized complex. For the [AlH4"HCl] complex (see **Figure 5.3**) this barrier has been calculated to be only 6.69 kcal/mol with an H(Al)-H(Cl) distance of 0.78 Å, just 0.03 Å longer than in free H₂ at the same level of theory.

For all the systems studied the net reaction is strongly exothermic,

Table 5.2, yielding H₂ and AlH₃A as products. The best candidate for
subsequent dynamic studies was considered to be [AlH₄...HCl] complex
because it has a small barrier for proton transfer, which at the same time is
much smaller than the association energy. Also the reverse reaction has a
huge barrier by comparison and competitive processes have far smaller
chances to happen. In order to check that the transition state connects the
reactant and the products, an intrinsic reaction coordinate (IRC) calculation,
steepest descent path in mass-weighed cartesian coordinates from the
transition state to both reactant and products, has been performed and the
result has been interpreted as a single step process, Figure 5.4.

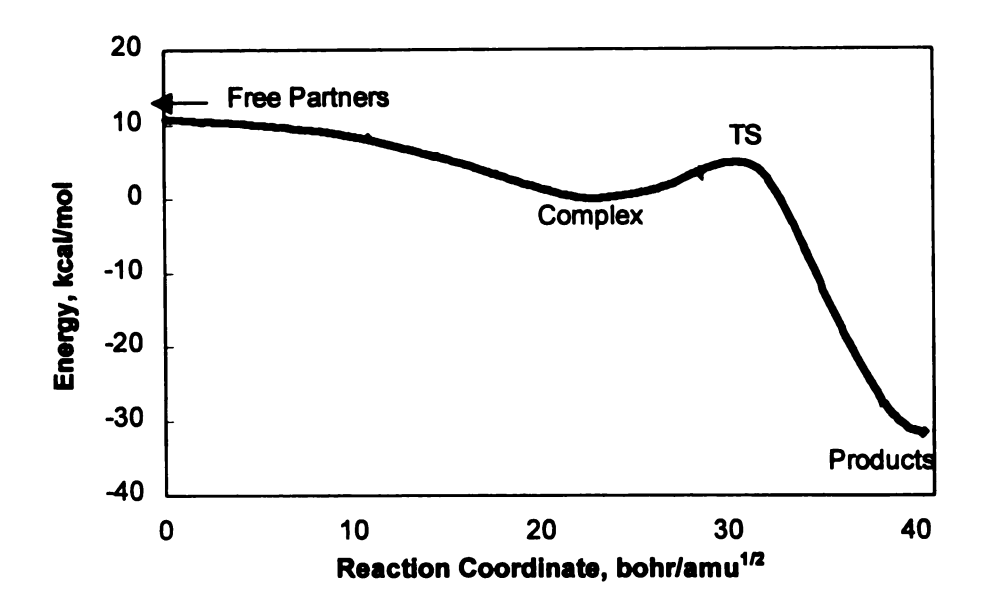


Figure 5.4 IRC Calculation for Proton Transfer and H₂ Loss in [AlH₄...HCl]⁻

2.2 Dynamics

Once the reactants, products, and transition state geometries were located on the PES, the reaction dynamics could be explored via ab initio classical trajectories. Among the modes associated with the dihydrogen bonded complex the ones relevant to proton transfer are 1411 and 1973 cm⁻¹, **Figure** 5.5.



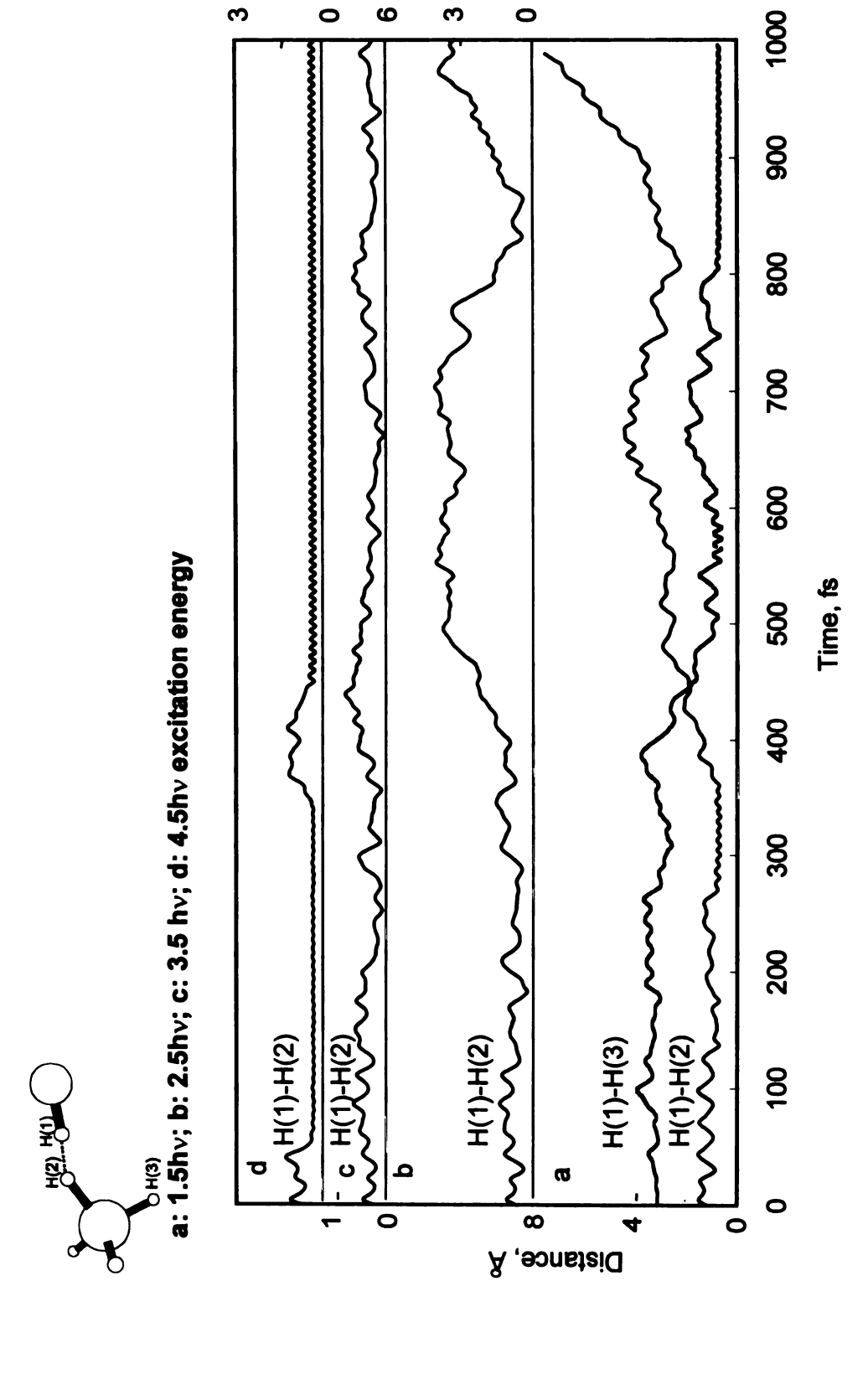
Figure 5.5 Excited Modes

These modes represent mixtures of symmetrical and antisymmetrical Al-H and Cl-H stretches involved in the H...H interaction.

In order to model the IRPR on [AlH4...HCl], we have performed dynamic reaction path (DRP) calculations. A method implemented in the GAMESS package, DRP allows for deposition of a selected energy quanta in a specific mode and classical treatment of the reaction dynamics, i.e. calculation of ab initio trajectories, as a result of this excitation.

The Al-H stretch, 1411 cm⁻¹, has been excited with different energies in the range 1.5-4.5 quanta, corresponding to 6.4-19.2 kcal/mol, and all the other modes with the ZPVE energy. It is important recognizing that with the first excitation energy, 6.4 kcal/mol, the system is brought close to the activation barrier, 6.69 kcal/mol, while in all the other situations the energy deposited is well above the activation barrier. The time evolution of the H(1)-H(2) distance, H(1) and H(2) are the proton and the hydride involved in dihydrogen bonding, is depicted in **Figure 5.6**. For 1.5 and 4.5 hv the proton transfer is followed by loss of the H₂ molecule within 400-800 fs via assistance from Cl⁻. The differences reside in the time scale for proton transfer and the hydrogen atom that is involved in the process.

Figure 5.6. Distance Evolution in Vibrationally Excited Complex at 1411 cm⁻¹



9

က

0

က

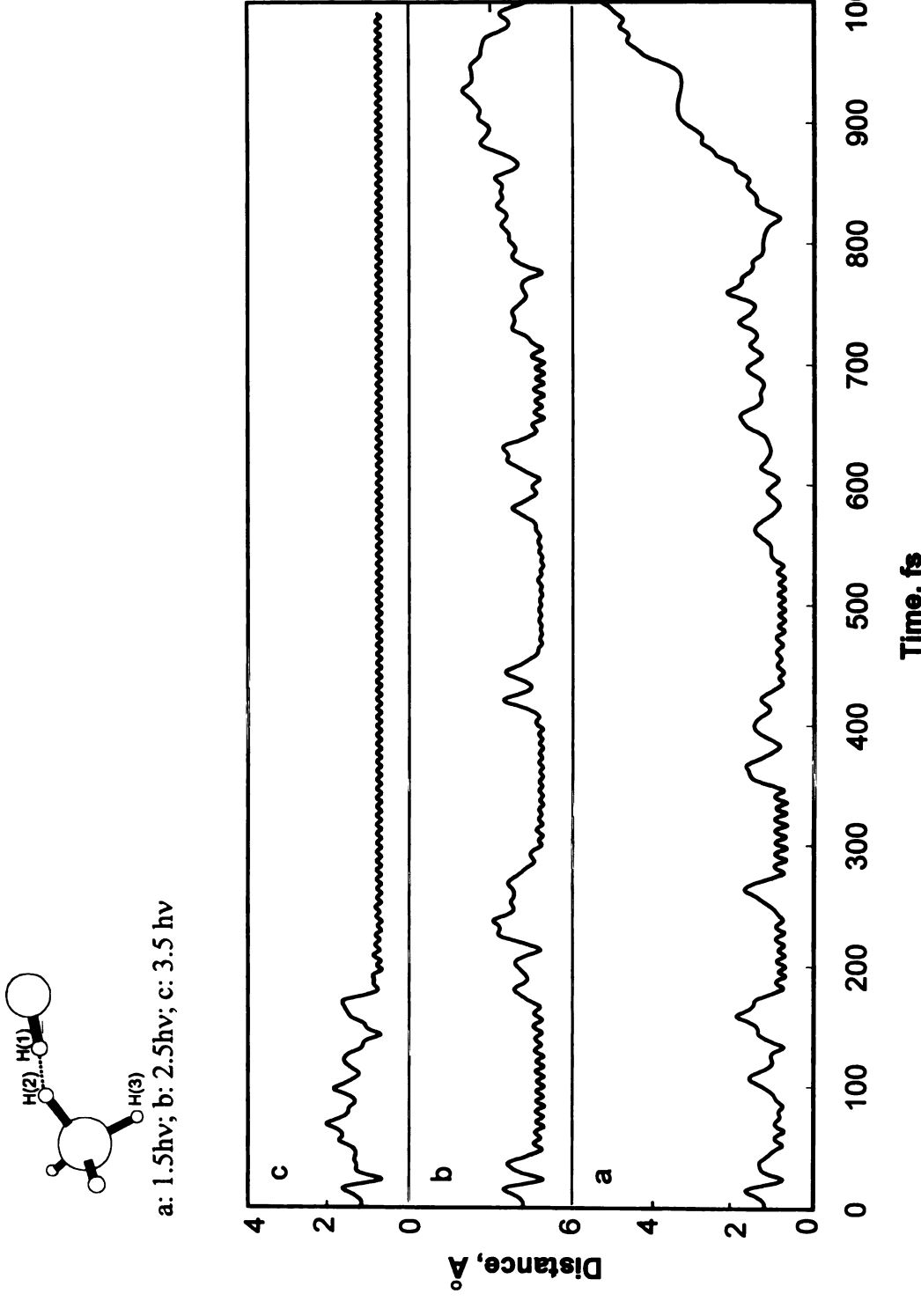
0

While for 4.5 quanta the particles that react are the ones that are dihydrogen bonded initially, for 1.5 quanta, the AlH₄ fragment rotates, moving a different hydride into position to interact with the proton and react to form H₂. For the intermediate energies, 2.5 and 3.5 quanta, the proton is transferred but undergoes reversion without liberation of H₂.

The H-Cl stretch, 1973 cm⁻¹, was excited with energies in the range 1.5-3.5 quanta, 9.0-22 kcal/mol, **Figure 5.6**. In all calculations proton transfer has been observed with the formation of complexed H₂ for time intervals that increased in length with the excitation energy. Only for 3.5 quanta, i.e. 22 kcal/mol, has H₂ loss accomplished within 200 fs. It is worth noting that in all simulations, for 1411 and 1973 cm⁻¹ modes, proton transfer, reversible or not, is observed.

It is of importance to know the extent of the reactant vibrational modes involvement in the proton transfer/H₂ loss reaction. In order to investigate this aspect we have performed a DRP calculation in which the starting point was the transition state with 0.05 kcal/mol energy deposited into the imaginary mode corresponding to the reaction path.

Figure 5.7 H(1)-H(2) Distance Evolution in Vibrationally Excited Complex at 1973 cm⁻¹



4

~

0

The amplitude and momentum of the modes were mapped onto the normal modes of the dihydrogen bonded complex, i.e. the ground state. In other words the normal modes of the reactant have been considered basis vectors to describe the reaction dynamics. The modes that we considered to be associated with the proton transfer, 1411 and 1973 cm⁻¹, were the only ones that at the ground state had amplitude changes characterized by periodicity, **Figure 5.8**, whereas the other were characterized by monotonic decay of amplitude, **Figure 5.9**.

Figure 5.8 Evolution of the 1411 and 1973 cm⁻¹ Modes Upon Transition

State Relaxation

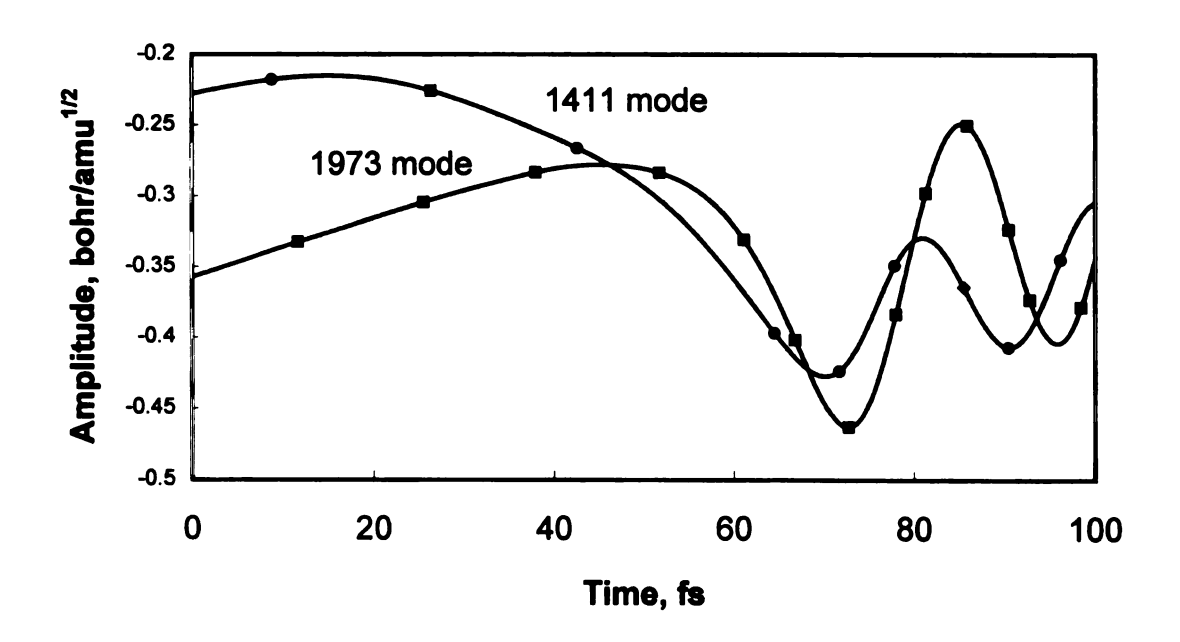
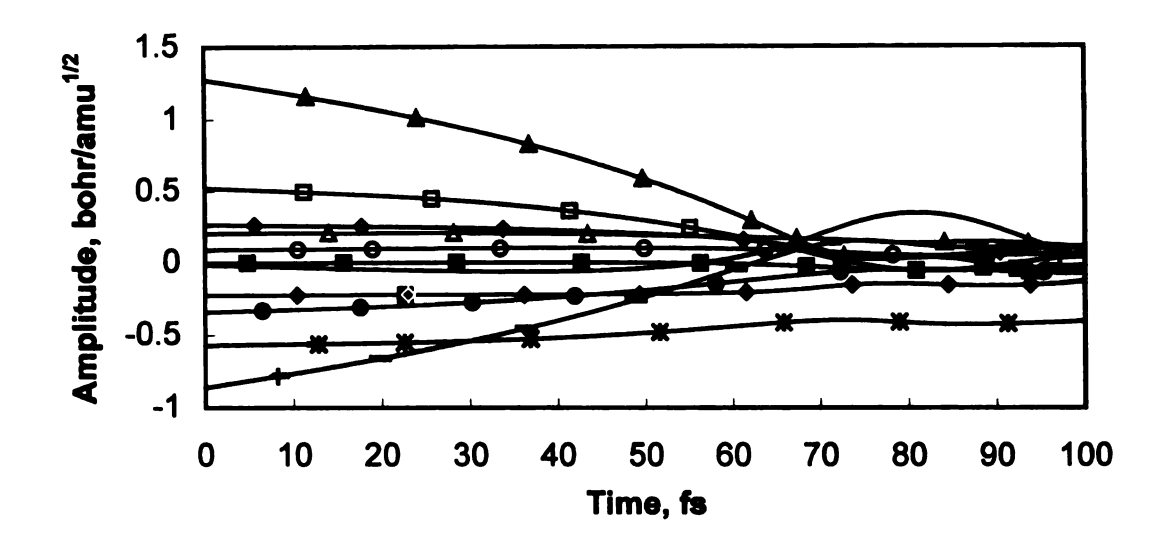


Figure 5.9 Evolution of the Modes Other Than 1411 and 1973 cm⁻¹
Upon Transition State Relaxation



Additional trajectories need to be computed in this 15-dimensional phase space but the rapid geometry and momentum changes require a small step size and consequentially long computational times, which do not readily allow for direct collection of statistically significant number of runs. However, the surprisingly general occurrence of proton transfer (albeit not always leading to dissociation of H₂) has been very encouraging for the potential of processes like theses for IRPR. It must be recalled that theses simulations are all classical. Presumably the contribution of tunneling would only serve to enable the reaction.

The particles involved in reaction are light and able to tunnel and we attempted to calculate a reaction rate based on the IRC, which includes tunneling correction based on a formalism presented by Cukier et al. 134 The IRC curve in cartesian coordinates has been fitted to a quartic potential, $V(r) = ar^2 + br^3 + cr^4$ (r is the reaction coordinate). The reactant well and barrier curvatures have been expressed as frequencies. The rate constant has been evaluated with and without an excitation energy found to be 0.836 ps⁻¹. Presence of an excitation energy of 6 kcal led as expected to an increase in the rate constant by 70 times. For values above the activation barrier the rate constant has reached a plateau around 0.086 fs⁻¹. For a more complete understanding we hope soon to be able to compute ab initio trajectories in which the hydride and the proton benefit from a quatum mechanical treatment, based on a new formalism¹³⁵ that will be introduced in the GAMESS package. 136

3. Kinetic and Mechanistic Investigations of

2-Hydroxycyclopentanone Reduction by Borohydride

Dihydrogen bonds have been at the core of extensive research since 1994. In the intervening years, their structures, and association energies have been explored, and their importance in reactivity and selectivity in solution and solid state have been demonstrated. Dihydrogen bonded complexes involving borohydrides are of particular importance – borohydrides are widely used as reducing agents.

Sharma, Huang, and Jackson have demonstrated the existence of H...H close contacts in the NaBH₄•H₂O crystal structure. Experimental and theoretical work by Epstein has also suggested the ability of borohydrides to dihydrogen bond with alcohols. Hydrolysis of BH₄⁻ in acidic or neutral conditions has been proven to involve proton transfer as rate determining step (RDS), followed by H₂ loss and B-O bond formation. The activation parameters, Δ H^{\pm} and Δ S^{\pm}, were determined to be 20.6 \pm 1 kcal/mol and – 22.3 \pm 3 e.u., for neutral conditions, and 8.0 \pm 1 kcal/mol and –3 \pm 3 e.u., for acidic hydrolysis, respectively. ¹³⁷⁻¹³⁹

Work done by S. Gatling in the Jackson group has aimed to explore the stereoselective control and reactivity enhancement facilitated by dihydrogen bonds in a typical borohydride reduction reaction. The

substrates, 2-hydroxycyclobutanone and 2-hydroxycyclopentanone, have been selected based on semiempirical calculations. Because of their ring frameworks, intramolecular hydrogen bond was thought to be unlikely in these structures and therefore rate enhancements or directing effects would not be expected from carbonyl activation by OH group. Also the chosen solvents, chlorinated hydrocarbons (1,2-dichlorobenzene and dichloromethane) and the borohydride's counterion, tetrabutyl ammonium, were unable to participate in hydrogen bonds with either the substrate or the borohydride. The results, summarized in **Table 6.1**, showed that the hydroxycycloalkanones were reduced at least 100 times faster than the corresponding simple cycloalkanones.

At the same time the analysis of the products has led to almost exclusively the trans diol product suggesting that the hydride is delivered from the OH substituted face of the substrate. The influence of competitive hydrogen bonding additives, and of replacement of the OH with a substituent incapable of hydrogen bonding were also studied.

We thought that it would be of interest to explore the influence of the dihydrogen bonding on the activation parameters of ketone reduction by tetrabutyl ammonium borohydride, NBu₄BH₄. We have chosen

2-hydroxycyclopentanone as substrate because it was the most thoroughly studied in the previous works.

Table 6.1. Reported Reduction Results of α -Hydroxycycloalkanones and of Corresponding Unsubstituted Ketones

Substrate	Solvent	t _{1/2}	Cis diol	Trans diol
◇= 0	DCB ^a	2 hrs		
OH_O	DCB ^a	<1 min	0.1	99.9
= 0	DCB	17 hrs		
OH OH	DCB	7 min	1.4	98.6
	CH ₂ Cl ₂	8 min	0.1	99.9

a: DCB = 1,2-dichlorobenzene

The overall ketone reduction reaction is given by the equation

$$4R_2C = O + NBu_4^{\bigoplus}BH_4^{\bigoplus} \longrightarrow NBu_4^{\bigoplus}[(R_2CHO)_4B]^{\bigoplus}$$
5.1

with the following steps:

$$R_2C=O + NBu_4 \ominus BH_4 \bigcirc \longrightarrow NBu_4 \ominus [R_2CHOBH_3] \bigcirc 5.2$$

$$R_2C=O+NBu_2^{\bullet}[R_2CHOBH_3]^{\bullet}$$
 $\longrightarrow NBu_2^{\bullet}[(R_2CHO)_2BH_2]^{\bullet}_{5.3}$

$$R_{2}C=O+NBu_{4}^{\bigoplus}[(R_{2}HCO)_{2}BH_{2}]^{\bigodot} \longrightarrow NBu_{4}^{\bigoplus}[(R_{2}CHO)_{3}BH]^{\bigodot} 5.4$$

$$R_{2}C=O+NBu_{4}^{\bigoplus}[(R_{2}CHO)_{3}BH]^{\bigodot} \longrightarrow NBu_{4}^{\bigoplus}[(R_{2}CHO)_{4}B]^{\bigodot} 5.5$$

Previous studies on ketone reductions by borohydrides have shown that the rate law is second order and that the intermediate species are more reactive that NBu₄BH₄. ¹⁴⁰ Wigfield and Gowland have examined the reduction of different ketones with a mixture of NaBH₄ and NaBD₄. The absence of isotopically mixed borohydride species at the end of the reaction, NaBH_nD_{4-n}, has been considered a proof that disproportionation has not taken place. ¹⁴¹

The OH from 2-hydroxycylopentanone and the borohydride, BH₄, are able to interact and thus a dihydrogen bonded complex is formed prior to the reduction. We have considered that the reaction has second order kinetics, first order in both ketone and borohydride, and that the rate determining step, RDS, is the transfer of the first hydride. The overall process is be described by **Scheme 6.1**.

Scheme 6.1

HO—
$$R_2C$$
—O + BH₄ — BH₄ — HO— R_2C —O HO— R_2HC —OBH₃ dihydrogen bonded complex
$$(HO-R_2HC - O)_4B$$
 cis and trans

The rate law is given by

$$\partial x/\partial t = k \cdot [ketone] \cdot [NBu_4BH_4]$$
 5.6

The ketone and borohydride concentrations were calculated as

$$[ketone]_t = [ketone]_0 - 4x$$
 5.7

$$[NBu4BH4]t = [NBu4BH4]0 - x$$
 5.8

where x is the conversion. Application of the above expressions in equation 5.6 led to

$$\partial x/\partial t = k \cdot \{ [ketone]_0 - 4x \} \cdot \{ [NBu_4BH_4]_0 - x \}$$
5.9

Integration of equation 5.9 gave

$$ln\{([NBu_4BH_4]_0 - x)/([ketone]_0 - 4x)\} = (4 \cdot [NBu_4BH_4]_0 - [ketone]_0)k \cdot t + ln([NBu_4BH_4]_0/[ketone]_0)$$
5.10

From the plot of $\ln\{([NBuBH_4]_0 - x)/([ketone]_0 - 4x)\}$ versus time the rate constant for a specific temperature was determined as

$$k = slope/(4 \cdot [NBu_4BH_4]_0 - [ketone]_0)$$
5.11

The Eyring equation gives the relationship between the activation parameters and the rate constant for a specific reaction:

$$k/T = k_B/h \cdot \exp(\Delta S^{\sharp}/R) \cdot \exp(-\Delta H^{\sharp}/R)$$
 5.12

From the logarithmic representation of the rate constant (k) versus (1/T) we obtained the activation enthalpy as

$$\Delta H^{\neq} = slope \cdot R$$
 5.13

$$\Delta S^{\neq} = \{ \text{intercept - ln}(k_B/h) \} \cdot R$$
 5.14

The reduction of 2-hydroxycyclopentanone was monitored at different temperatures over a range of 40 K by solution IR spectroscopy. The concentrations of ketone and borohydride were 0.1 and 0.4 M, respectively, to ensure an excess of the reducing agent at all times. The progress of the reaction was followed via the carbonyl's absorption. We determined the concentration of ketone during the reaction using a calibration line based on the carbonyl peak (1748.6 cm⁻¹). The borohydride concentration was determined with the help of equation 5.7 and 5.8. The OH peak, which was observed at 3450 cm⁻¹ in a solution of ketone in 1,2-dichlorobenzene (1,2 DCB), shifted to 3250 cm⁻¹, indicative of a dihydrogen bonding interaction, in the presence of borohydride and its appearance remained unchanged during the reaction. Through all the runs we did not observed H₂ evolution. As expected the reaction kinetics were found to be first order in ketone (see Figure 6.1) and in borohydride (see Figure 6.2).

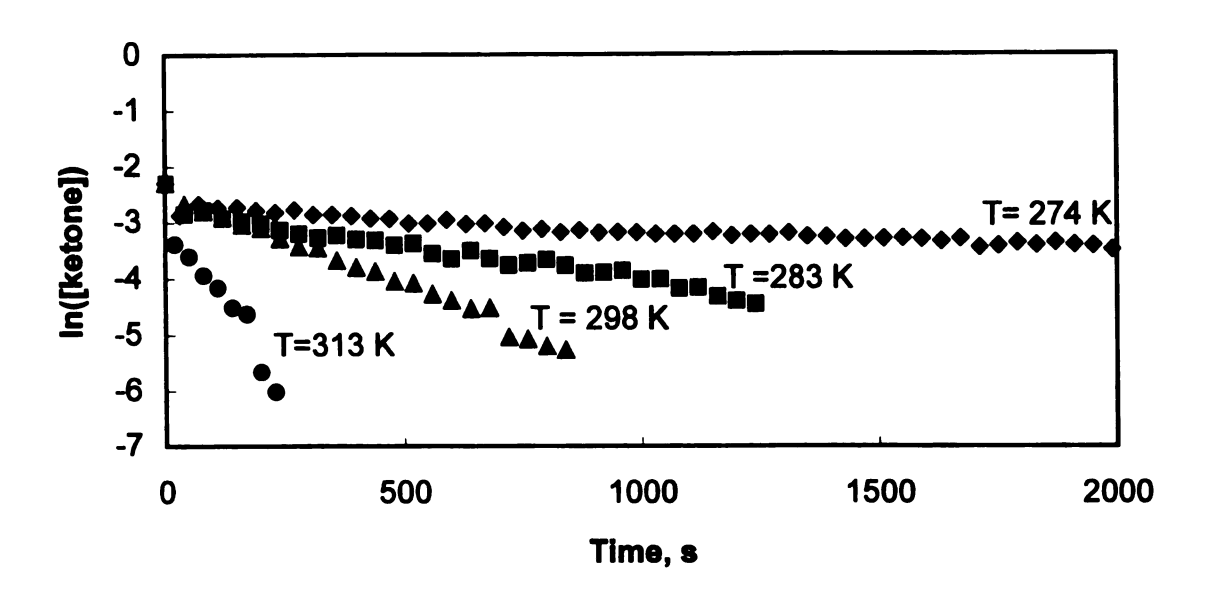


Figure 6.1 Time Evolution of Ketone Concentration

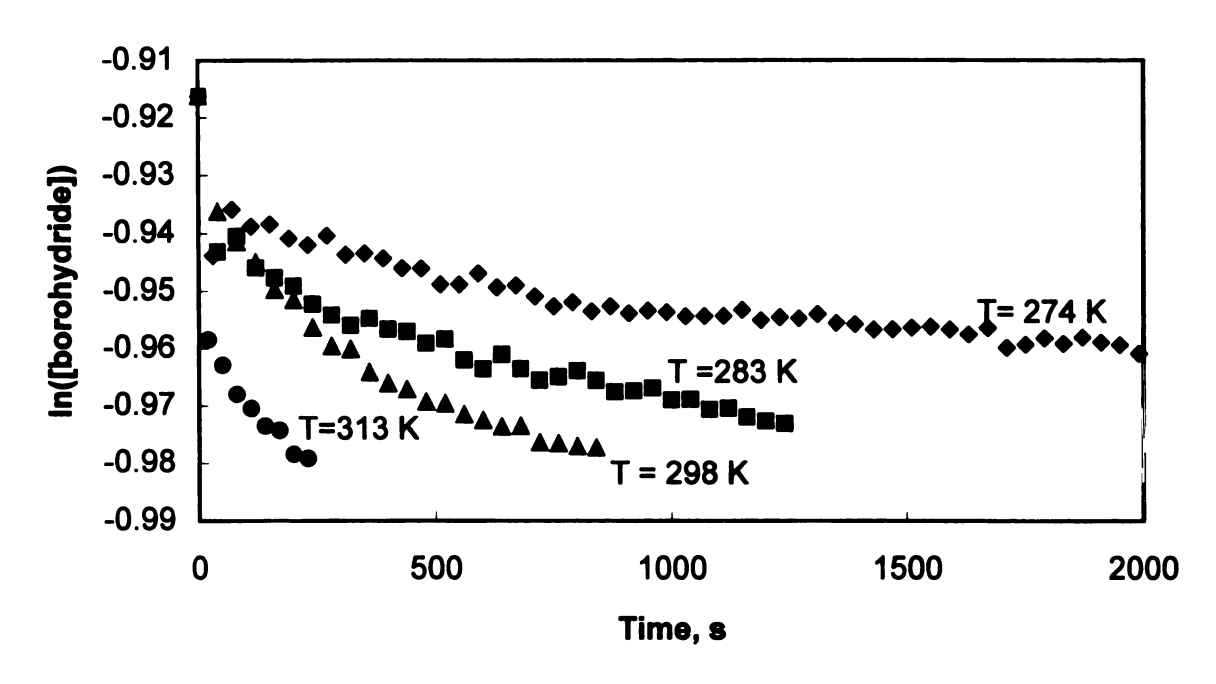


Figure 6.2 Time Evolution of Borohydride Concentration

Application of the ketone and borohydride concentrations in equation 5.10 allowed us to obtain the integrated rate laws that have been depicted in Figure 6.3.

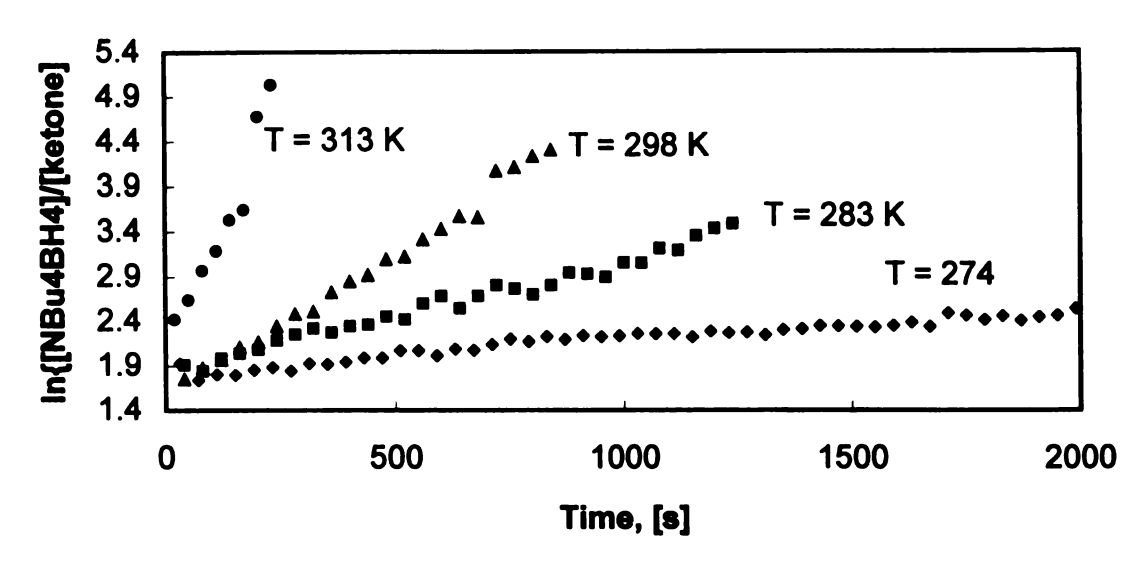


Figure 6.3 Integrated Rate Laws for Reduction of

2-Hydroxycylopentanone by NBu₄BH₄

Using equation 5.11, we have determined the rate constants, and their values have been summarized in **Table 6.2**.

Table 6.2. Rate Constants for the Reduction of 2-Hydroxycyclopentanone by NBu₄BH₄

Temperature, K	k, [l·mol ⁻¹ ·s ⁻¹] · 10 ³	
274	0.33 ± 0.027	
283	1.00 ± 0.033	
298	2.20 ± 0.160	
315	8.10 ± 0.890	

The representation of equation 5.12 has been depicted in **Figure 6.4** and the activation parameters have been determined using the equations 5.13 and 5.14 (**Table 6.3**)

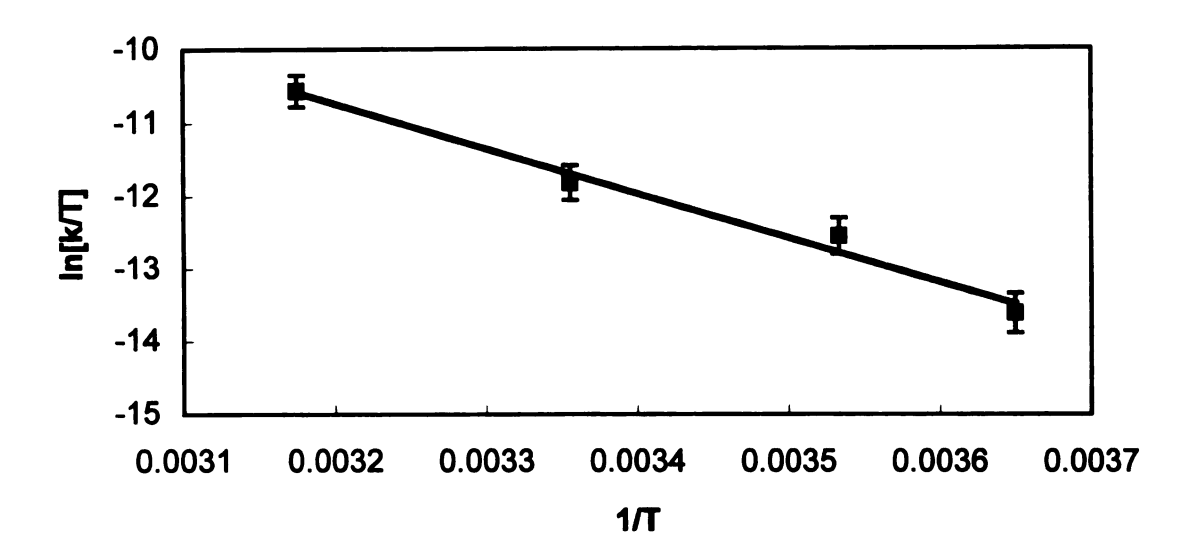


Figure 6.4 Logarithmic Representation of the Eyring Equation

For comparison the reduction of cyclopentanone by NBu₄BH₄ in 1,2-dichlorobenzene and in 2-propanol have also been performed and the activation parameters have been determined (**Table 6.3**).

Dihydrogen bonding between the OH substituent and BH₄⁻ lowers the enthalpy of activation by 6.6 kcal. A larger effect on the enthalpy is observed when the solvent is 2-propanol. While in the 2-hydroxycyclopentanone/BH₄⁻ system there is one dihydrogen bond, in the cyclopentanone/BH₄⁻/2-propanol there one hydrogen bond between the carbonyl and the OH from the alcohol and dihydrogen bonds between the

BH₄ and 2-propanol. Thus activation of both carbonyl and borohydride will lower the activation enthalpy of the reaction. At the same time the presence of interactions requires a higher degree of organization in the transition state, more so when there is an excess of proton donors, and hence the larger negative value for the activation entropy.

Table 6.3. Activation Parameters for Ketones Reductions

Substrate	Solvent	ΔH^{\neq} , [kcal/mol]	$\Delta \mathbf{S}^{\neq}$, [e.u.]
OH →□	DCB	12.2 ± 1.89	-29.6
	DCB	18.8 ± 1.08	-22.9
	2-iPrOH	9.8 ± 1.07	-44.3

We were interested in further investigating the influence of different factors on the stereochemical outcome. When we used the same work-up procedure employed by dr. S. Gatling and analysis by gas chromatography we were able to reproduce the results previously obtained for the 2-hydroxycyclopentanone/NBu₄BH₄ system in dichloromethane. It is of importance to note that the actual work-up procedure is different from the one reported. Instead of the H₂O₂/NaOH quenching followed by dichloromethane extraction of the aqueous layer and concentration (which

was the reported work-up) we treated the reaction mixture with HCl, followed by neutralization of the aqueous layer and removal of water (procedure used by dr. S. Gatling). ¹⁴² In both procedures the alcohols mixtures were derivatized to the corresponding trimethylsilyl ethers and were analyzed by gas chromatography.

Equipment upgrade in our laboratories allowed us to examine the products of reaction directly via HPLC. We analyzed the different layers of the reaction mixture at each step in the work-up procedure and we noted that there were losses at each step. Moreover the trans and cis diols were not hydrolyzed to the same extent and also were not extracted with the same efficiency, (see **Table 6.4**).

Table 6.4 Work-up Procedures Results

Work-up	Layer	Trans*	Cis ^a	Diols ^b
H ₂ O ₂ /NaOH	H ₂ O	52	48	51
	CH ₂ Cl ₂	81	19	49
6N HCl	H_2O	97	3	43
	CH ₂ Cl ₂	45	55	57

a.% of cis or trans diol in the respective layer

We used instead a single step procedure without separation or derivatization, treatment with concentrated H₂SO₄. The results are

b. % of diols (cis and trans) in the respective layer

summarized in **Table 6.5** together with the ones previously obtained by S. Gatling. We observed a smaller directing effect, trans:cis ratio 63:37 as opposed to 99.7:0.3 reported by dr. S. Gatling in similar conditions. One reason for the discrepancy in the results is the stability of the cyclic borates corresponding to the 1,2 cis diol. The equilibrium constant was determined to be 1.9 in favor of the borates formed by the 1,2 cis hexanediol. Also in the acidic work-up the aqueous layer has a much smaller volume than the organic layer and 15 ml CH₂Cl₂ and thus hydrolysis of the borates is not favored.

In order to clarify if the lower trans:cis ratio observed could be attributed solely to the reduced number of separation steps, we have run the reaction at higher dilution and lower temperature, and we observed that the trans diol is slightly favored. This result was interpreted as evidence of the increased ability of the dihydrogen bonded complex to react at low temperature and high dilution before the intermediate alkoxyborohydride species participate in reaction.

Subsequent ab initio calculations at the B3LYP/6-311G level found that 2-hydroxycylopentanone is in fact capable of intramolecular hydrogen bonding, despite Jackson and Gatling earlier assumption to the contrary,

Figure 6.5. We calculated a O-H...O(=C) close contact of 2.35 Å and an OH

frequency shift of 65 cm⁻¹ compared to the non hydrogen bonded conformer. The hydrogen bonded structure was found to be more stable by 4.8 kcal/mol.

Table 6.5 Trans: Cis Ratios in 2-Hydroxycyclopentanone Reduction

[Ketone]	[BH ₄ -]	[Trans]	[Cis]	Additive
0.321 ^a (0.25)	0.356	62.8 (99.7)	37.2 (0.3))
0.163 ^a	0.500	62.4	37.6	
0.078 ^a	0.016	72.6	27.4	
0.140 ^b	0.132	71.7	28.3	
0.008 ^a	0.531	62.0	38.0	
0.011 ^a	0.012	65.6	34.4	
0.013 ^a	0.013	72.0	27.0	
0.005 ^a	0.005	69.2	30.8	
0.004 ^b	0.002	79.6	20.4	
0.349 ^a (0.25)	0.331 (0.25)	63.5 (93.5)	36.5 (6.5)	TBABr
0.357 ^a (0.25)	0.324 (0.25)	64.2 (79.7)	35.8 (20.3) TBACI
0.376 ^a (0.25)	0.310 (0.25)	65.8 (54.5)	34.2 (45.5) TBAF
0.242 ^c	0.250	70.0	30.0	
0.242 ^d	0.250	46.5	53.5	

a: NBuBH₄, CH₂Cl₂

The values in parenthesis are previously reported results.

b: temperature 0 °C

c: NaBH₄, THF

d: LiBH₄, THF

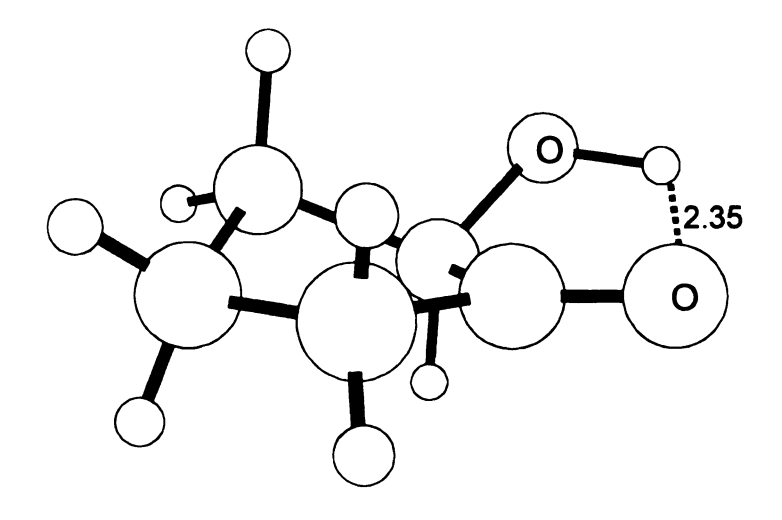


Figure 6.5 2-Hydroxycyclopentanone

When BH₄ was introduced into the calculations we have been able to find two minima for the optimized dihydrogen bonded complexes.

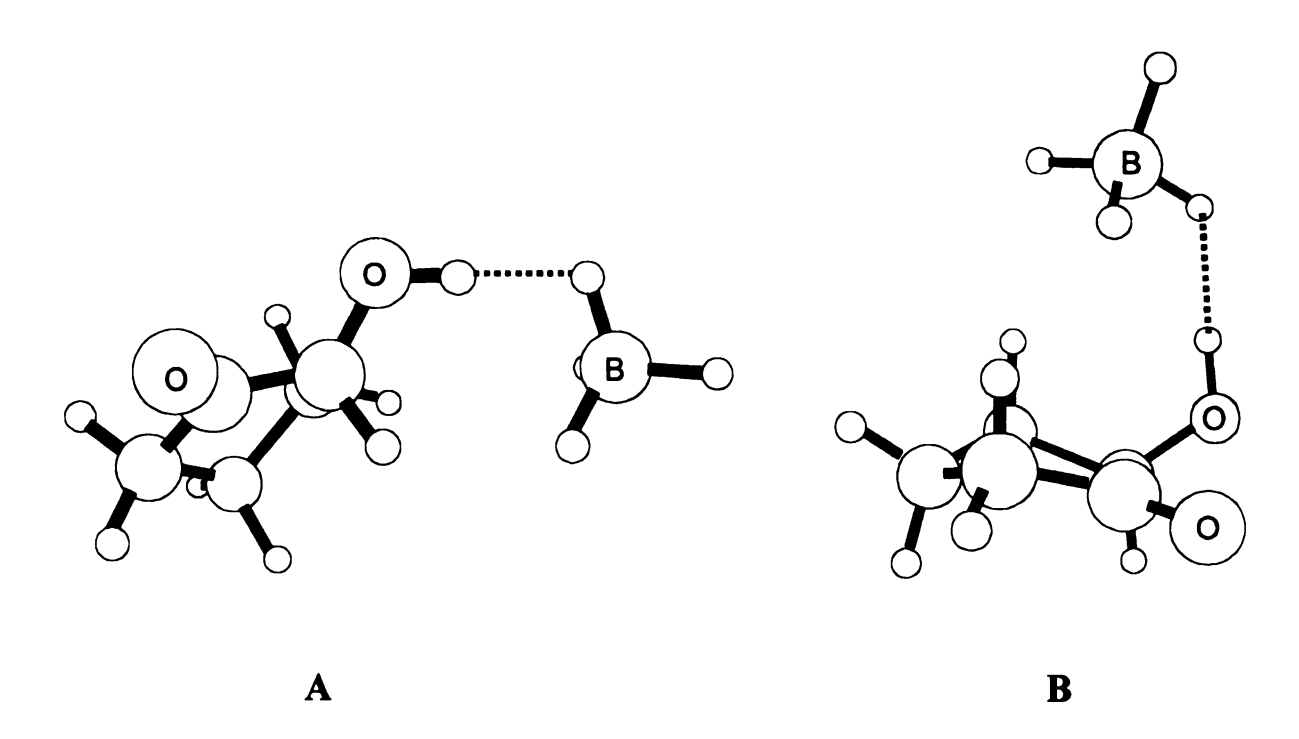


Figure 6.6 2-Hydroxycyclopentanone·BH₄ Complexes

In the structure with the lowest energy, the BH₄ ion lies almost in the plane of the ring suggesting a small face selectivity for the reduction. The structure

that has the BH₄ coming from the OH substituted face of the ring, **B** in Figure 6.6, is higher in energy by 0.7 kcal/mol.

Presence of additives capable of hydrogen bonding to the ketone's OH should be able to slow the reaction rate and decrease selectivity as a result of competing with the BH₂ for interaction with the OH. Dr. Gatling's reported that addition of tetrabutylammonium bromide (TBABr). tetrabutylammonium chloride (TBACl), and tetrabutylammonium fluoride (TBAF) decreased the reaction rate and the trans: cis ratio of the diols in the order TBABr<TBACl<TBAF in accordance with Br'<Cl'<F' trend as hydrogen bond partners. We have observed in similar conditions barely any influence. Based on the structure that we have obtained for the dihydrogen bonded complex. A in Figure 6.6, one explanation may be that the hydrogen bonded complex adopts a conformation with the X'(X = Br, Cl, F) in the plane of the ring also. Also dr. Gatling used all TBAX without purification and in their commercial form they contain water, which is a very good dihydrogen bonding partner for the borohydride, in other words the change in the reaction rate cannot be attributed only to the TBAX. In our set of experiments we used recrystallized TBAX (water removal was checked via IR).

We chose NBu₄BH₄ to study the reduction of ketones by borohydrides because the counterion, NBu₄⁺, is incapable of hydrogen bonding to either substrate or borohydride. However in practical synthetic organic chemistry the widely used borohydrides are NaBH₄ or LiBH₄ in solvents such as tetrahydrofuran (THF) and we were interested to explore the streochemistry of the reaction in those conditions. The trans:cis ratio was dictated by the solubility of the borohydrides; for NaBH₄ which has a lower solubility, the ratio was essentially the same as in the system NBu₄BH₄/CH₂Cl₂, but for more soluble LiBH₄, an almost equimolar trans:cis ratio was observed.

4. Methods of Calculation

The methods presented in this chapter refer to the calculations from chapter 2. Calculations used the MP2 level of theory and the 6-311++G** basis set within GAUSSIAN 94,144 GAUSSIAN 98145 and GAMESS146 packages. Complexes were obtained by optimizing a structure with the hydride, AlH₄, and the proton donor, HA, initially at large distance. H...H contact distances smaller than 2.4 Å and association energy were used as criteria o validate or refute a dihydrogen bonded complex. The interaction energy was calculated as the difference between the complex's energy and the sum of the free partners' energies including the zero point vibrational energy corrections. Because previous calculations in the Jackson group had shown this level of theory to be quantitatively successful in estimating halide and borohydride ion-molecule association energies, we did not correct for basis set superposition error (BSSE). Vibrational analyses were performed to confirm the nature of all stationary points on the PES, i. e. the dihydrogen bonded complexes were minima with no imaginary frequencies.

The potential energy surface (PES) for the proton transfer/H₂ loss reaction was investigated via a relaxed scan with respect to the proton-hydride distance. The H...H distance was stepped from the value in the dihydrogen bonded complex to the value in the H₂ molecule and at each

selected distance all the other parameters were reoptimized. A vibrational analysis was performed on the highest energy structure to confirm/refute its transition state nature, i.e. one imaginary frequency corresponding to proton transfer. Subsequently the structure was reoptimized as a transition state.

The last structure from the PES relaxed scan was fully optimized and considered the product geometry. The intrinsic reaction coordinate (IRC), steepest descent path in mass-weighted coordinates calculation, was then traced in order to verify the concerted or step-wise nature of the process and also to check that the transition state connects the reactant and products.

Once the most suitable candidate ([AlH4...HCl]) for IRPR was found, the modes associated with the proton transfer were identified and a series of dynamics studies was performed using the dynamic reaction path (DRP)¹⁴⁷ method implemented in the GAMESS package. DRP method allows for deposition of excitation energy in a specific vibrational and calculation of classical ab initio trajectories resulted from that excitation. Two types of DRP calculations were done. First we deposited in each of the modes associated with proton transfer in the dihydrogen bonded complex, i. e. ground state, variable amounts of energy while all the other modes had ZPVE energy and analyzed the reaction dynamics. We also excited the transition state with 0.05 kcal/mol and investigated the energy transfer as the

system relaxed to the dihydrogen bonded complex. The excitation energy was deposited in the imaginary mode corresponding to the reaction path and the amplitude and momenta of the modes were mapped onto the normal modes of the dihydrogen bonded complex.

For the tunneling corrections a new IRC calculation, in cartesian coordinates, was performed and the curve was fitted to a quartic potential:

$$V(r) = ar^2 + br^3 + cr^4$$

The microscopic rate constant was defined as

$$k[E] = (\tau[E])^{-1}e^{-S[E]/\hbar}$$

where, E is the excitation energy. The well vibrational period, $\tau[E]$, and the semiclassical action, S[E], were given as

$$\tau[E] = 2(m/2)^{1/2} \int [E-V(r)]^{-1/2} dr$$

$$S[E]/\hbar = 2(2m)^{1/2}/\hbar \int \{ [V(r)-E] dr \}^{1/2}$$

For the quartic potential, the reactant well curvature was defined by

$$\omega_0 = [V''(r)_{r=r0}/m]^{1/2}$$

where r0 is the position of the reactant well minimum. The barrier curvature, ω_b was expressed as

$$\omega_b = [V''(r)_{r=0}/m]^{1/2}$$

The barrier height was defined by

$$Vb = V(r = 0) - V(r = r0)$$

Application of all the above expressions led to the rate constant

$$k[E] = \omega_0/(2\pi) exp\{-2\pi[Vb\text{-}E]/(\hbar\omega_b)\}$$

and when the excitation energy became close to the barrier

$$k[E] = \omega_0 / \{2\pi \{1 + \exp\{2\pi [Vb-E]/(\hbar \omega_b)\}\}\}$$

The above equations were used to calculate the rate constants when different excitation energy values were considered.

5. Experimental Section

General

All reagents were purchased from commercial sources and purified when necessary. Reductions were monitored by FTIR using a REACT IR MP Mobile spectrometer. Calibration curves were obtained for all reactants. The cis/trans diol ratios were analyzed by HPLC.

HPLC Column Characteristics:

Name: BIORAD Aminex HPX-87H

Conditions - mobile phase: 5 mM H₂SO₄ solution

- low rate: 0.6 ml/min

- temperature: 65 °C

- detector: UV 210 nm

RI

- injection size: 10 μl

Kinetic Studies of Reductions with Tetrabutylammonium Borohydride.

Standard solutions of 2-hydroxycyclopentanone (0.2M) and tetrabutylammonium borohydride (0.8M) in 1,2-dichlorobenzene were prepared. The solvent was purchased dry from Aldrich.

Tetrabutylammonium borohydride was recrystallized from ethyl acetate and dried under vacuum for 24 h at room temperature. In a 50 ml three-neck

round bottom flask fitted with a magnetic stirring bar, a reflux condenser connected to a nitrogen line, and a thermometer, 10 ml of the tetrabutylammonium borohydride solution was placed and allowed to thermally equilibrate. After the desired temperature was reached, 10 ml of the ketone solution (kept at the same temperature) was added and the IR spectra were recorded beginning 20 seconds after the mixing and at intervals determined by the reaction length at a specific temperature.

When the carbonyl compound was cyclopentanone, to 20 ml solution of tertabutylammonium borohydride (0.6M), 1.4 ml (0.016 moles) cyclopentanone were added. Cyclopentanone was purchased from Aldrich and redistilled at (bp = 130°C) at atmospheric pressure under nitrogen.

¹H NMR (CDCl₃, 300 MHz): 1.66, multiplet (4H); 1.95, multiplet (4H). IR: 1746 cm⁻¹ (CO).

Preparation of 2-hydroxycyclopentanone¹⁴⁸

A. 1,2-Bis(trimethylsilyloxy)cyclopentene.

A 1 liter, three-neck flask was fitted with a mechanical stirrer, a dropping funnel, a reflux condenser and maintained under an oxygen-free, nitrogen atmosphere. The flask was charged with 300 g reagent grade toluene (dried over MgSO₄) and 15 g freshly cut sodium. The temperature was slowly increased to 110°C. The stirrer was operated at full speed to disperse the

sodium. A mixture of 75 g (0.69 mole) chlorotrimethylsilane, and 24 g (0.15 mole) dimethyl glutarate in 50 ml toluene was added over 3 hours. After reacting for 12 hours, the mixture was cooled and filtered. The precipitate was washed several times with anhydrous diethyl ether. Toluene was removed under reduced pressure and the crude 1,2-

bis(trimethylsilyloxy)cyclopentene was vacuum distilled, b.p. 53°C (0.3 mm Hg), (22.5 g, 61.1%). H NMR (CD₂Cl₂, 300 MHz): 0.2, multiplet (18H); 1.0-2.0, multiplet (6H).

B. 2-Hydroxycyclopentanone.

In a 250 ml, three neck flask fitted with a magnetic stirrer, a dropping funnel, a nitrogen bubbler and a reflux condenser, 115 ml reagent grade methanol was placed. Dry oxygen-free nitrogen was vigorously bubbled through the methanol for 1 hour. The 22.5 g of

1,2-bis(trimethylsilyloxy)cyclopentene were added dropwise for 2 hours at room temperature. The methanol and methoxytrimethylsilane were removed under reduced pressure, the crude 2-hydroxycyclopentanone was dissolved in 10 ml water and a catalytic amount of concentrated H₂SO₄ was added. After reacting for 6 hours the 2-hydroxycyclopentanone was extracted with 3 x 10 ml CH₂Cl₂. The solution was dried (over MgSO₄) and the solvent was removed under reduced pressure and the

2-hydroxycyclopentanone was vacuum distilled, b.p. 43°C, (0.9 mm Hg), (5.6 g, 56%). IR: 3415 cm⁻¹ (OH), 1746 cm⁻¹ (CO); ¹H NMR (CD₂Cl₂, 300 MHz): 4.03, triplet (1H); 3.02, singlet, broad (1H); 1.5-2.5, multiplet (6H) Cis/trans diols Ratio Analysis

Standard solutions of carbonyl (0.5M) and tetrabutylammonium borohydride (0.5M) in CH₂Cl₂ (dried over P₂O₅) were prepared. 0.5 ml of each solution were added to a vial, shaken well, and then allowed to react for up to 6 hours. Out of each reaction mixture 0.1 ml were taken and treated with concentrated H₂SO₄ and diluted up to 1 ml with the mobile phase that had as internal standard ethylene glycol (0.25M). The additives tetrabutylammonium fluoride (dried under reduced pressure at 70°C for 24 hrs), tetrabutylammonium chloride (recrystallized from CH₂Cl₂/Et₂O) and tetrabutylammonium bromide (recrystallized from CH₂Cl₂/Et₂O) were added to the ketone solution before the addition of the tetrabutyl ammonium borohydride solution. NaBH₄ was recrystallized from i-PrOH/CH₂Cl₂, tetrahydrofuran was dried over P₂O₅ and LiBH₄ used as purchased.

BYBLIOGRAPHY

- 1. Oref, L.; Rabinovitch, B. S. Acc. Chem. Res. 1979, 12, 166.
- 2. Zewail, A. H. Phys. Today 1980, 33, 27.
- 3. Zewail, A. H. Acc. Chem. Res. 1980, 13, 360.
- 4. King, D. S.; Hochstrasser, R. M. J. Am. Chem. Soc. 1975, 97, 4760.
- 5. Reddy, K. V.; Berry, M. J. Chem. Phys. Lett. 1979, 66, 223.
- 6. Hall, R.; Kaldor, A. J. Chem. Phys. 1979, 70, 4027.
- 7. Lupo, D. W.; Quack, M. Chem. Rev. 1987, 87, 181.
- 8. Baumert, T.; Helbing, J.; Gerber, G. Adv. Chem. Phys. 1997, 101, 47.
- 9. Scherer, N. F.; Carlson, R. J.; Matro, A.; Ruggiero, M. Du; Romero-Rochin, V.; Cina, J. A.; Fleming, G. R.; Rice, S. A. J. Chem. Phys. 1991, 95, 1487.
- 10. Shapiro, M.; Brumer, P. Chem. Phys. 1989, 139, 221.
- 11. Shapiro, M.; Brumer, P. J. Chem. Phys. 1986, 84, 4103.
- 12. Shapiro, M. Brumer, P. Acc. Chem. Res. 1989, 22, 407.
- 13.Fiss, J. A.; Zhu, L. C.; Suto, K.; He, G. Z.; Gordon, R. J. Chem. Phys. 1998, 233, 335.
- 14.Zhu, I.; Suto, K.; Fiss, J. A.; Wada, R.; Seideman, T.; Gordon, R. J. *Phys. Rev. Lett.* **1997**, *79*, 4108.
- 15. Shapiro, M.; Chen, Z.; Brumer, P. Chem. Phys. 1997, 217, 325...
- 16. Chen, Z.; Brumer, P.; Shapiro, M. Chem. Phys. Lett. 1992, 198, 498.
- 17. Kobrak, M. N.; Rice, S. A. Phys. Rev. A 1998, 57, 2885.

- 18. Kobrak, M. N.; Rice, S. A. J. Chem. Phys. 1998, 109, 1.
- 19. Shnitman, A.; Sofer, I.; Golub, I.; Yogev, A.; Shapiro, M.; Chen, Z.; Brumer, P. Adv. Chem. Phys. 1997, 101, 285.
- 20. Shnitman, A.; Sofer, I.; Golub, I.; Yogev, A.; Shapiro, M.; Chen, Z.; Brumer, P. *Phys. Rev. Lett.* **1996**, *76*, 2886.
- 21. Abrashkevich, D. G.; Shapiro, M.; Brumer, P. J. Chem. Phys. 2002, 116, 5584.
- 22. Pierce, A. P.; Dahleh, M. A.; Rabitz, H. Phys. Rev. A 1988, 37, 4950.
- 23. Shi, S. H.; Woody, A.; Rabitz, H. J. Chem. Phys. 1988, 88, 6870.
- 24.Shi, S. H.; Rabitz, H. J. Chem. Phys. 1990, 92, 364.
- 25. Judson, R. S.; Rabitz, H. Phys. Rev. Lett. 1992, 68, 1500.
- 26. Gross, P.; Neuhauser, D.; Rabitz, H. J. Chem. Phys. 1993, 98, 4557.
- 27. Toth, G. J.; Lorincz, A.; Rabitz, H. J. Chem. Phys. 1994, 101, 3715.
- 28. Phan, M. Q.; Rabitz, H. Chem. Phys. 1997, 217, 389.
- 29. Phan, M. Q.; Rabitz, H. J. Chem. Phys. 1999, 110, 34.
- 30. Geremia, J. M.; Zhu, W. S.; Rabitz, H. J. Chem. Phys. 2000, 113, 10841.
- 31. Lewis, R. J.; Menkir, G. M.; Rabitz, H. Science 2001, 292, 709.
- 32. Assion, A.; Baumer, T.; Bergt, M.; Brixner, T.; Kiefer, B.; Seyfried, V.; Strehle, M.; Gerber, G. Science 1998, 282, 919.
- 33.Brixner, T.; Damarauer, N. H.; Niklaus, P.; Gerber, G. *Nature* **2001**, 414, 57.

- 34. Henriksen, N. E. Chem. Soc. Rev. 2002, 31, 37.
- 35. Althorpe, S. C.; Fernandez-Alonso, F.; Bean, B. D.; Ayers, J. D.; Pomerantz, A. E.; Zare, R. N.; Wrede, E. *Nature* **2002**, *416*, 67.
- 36. Heiweil, E. J.; Casassa, M. P.; Cavanagh, R. R.; Stephenson, J. C. J. Chem. Phys. 1986, 85, 5004.
- 37. Graener, H.; Ye, Q.; Laubereau, A. J. Chem. Phys. 1989, 90, 3413.
- 38. Graener, H.; Ye, Q.; Laubereau, A. J. Chem. Phys. 1989, 91, 1043.
- 39. Ye, Q.; Graener, H. J. Phys. Chem. 1989, 93, 5963.
- 40.Liddel, U.; Becker, D. E.; Spectrochimica Acta 1957, 10, 70.
- 41. Biondi, A.; Simkin, D. J. J. Chem. Phys. 1956, 25, 1073.
- 42. Laenen, R.; Rauscher, C.; Laubereau, A. J. Phys. Chem. A 1997, 101, 3201.
- 43. Barnes, A. J.; Hallam, H. E. Trans. Faraday Soc. 1970, 66, 1932.
- 44. Laenen, R.; Rauscher, C. J. Chem. Phys. 1997, 106, 8974.
- 45. Laenen, R.; Rauscher, C. J. Mol. Struct. 1998, 448, 115.
- 46. Woutersen, S.; Emmerichs, U.; Bakker, H. J. J. Chem. Phys. 1997, 107, 1483.
- 47. Coussan, S.; Bakkas, N.; Loutellier, A.; Perchard, J. P.; Racine, S. Chem. Phys. Lett. 1994, 217, 123.
- 48.Bonn, M.; Bakker, H. J.; Kleyn, A. W.; van Santen, R. J. Phys. Chem. 1996, 100, 15301.
- 49.Iwaki, L. W.; Dlott, D. D. J. Phys. Chem. A 2000, 104, 9101.

- 50.Levinger, N.; Davis, P. H.; Fayer, M. D. J. Chem. Phys. 2001, 115, 9352.
- 51. Gaffney, K. J.; Piletic, I. R.; Fayer, M. D. J. Phys. Chem. A 2002, 106, 9428.
- 52. Gaffney, K. J.; Davis, P. H.; Piletic, I. R.; Levinger, N. E; Fayer, M. D. J. Phys. Chem. A 2002, 106, 12012.
- 53. Bakker, H. J.; Woutersen. Phys. Rev. Lett. 1999, 83, 2077.
- 54. Kropman, M. F.; Nienhuys, H. -K.; Woutersen, S.; Bakker, H. J. J. Phys. Chem. A 2001, 105, 4622.
- 55. Nienhuys, H. -K.; Lock, A. J.; van Santen, R.; Bakker, H. J. J. Chem. Phys. 2002, 117, 8021.
- 56.Rey, R.; Moller, K. B.; Hynes, J. T. J. Phys. Chem. A 2002, 106, 11994.
- 57. Strauss, H. L. Acc. Chem. Res. 1997, 30, 37.
- 58.Cha, Y.-H.; Strauss, H. L. J. Phys. Chem. A 2002, 106, 3531.
- 59. Choi, C. –H.; Kuwata, K. T.; Cao, Y. –B.; Okumura, M. J. Phys. Chem. A 1998, 102, 503.
- 60. Schriver, A.; Racine, S.; Schrems, O.; Schriver-Mazzuoli, L. Spectrochimica Acta 1994, 50A, 287.
- 61. Schriver, L.; Schriver, A.; Perchard, J. -P. J. Mol. Struct. 1990, 222, 141.
- 62. Giebels, I. A. M. E.; van der Broek, M. A. F. H.; Kropman, M. F.; Bakker, H. J. J. Chem. Phys. 2000, 112, 5127.

- 63. Custelcean, R.; Jackson, J. E. Chem. Rev. 2001, 101, 1963.
- 64. Epstein, L. M.; Shubina, E. S. Coordin. Chem. Rev. 2002, 231, 165.
- 65. Brown, M.P.; Walker P. J. Spectrochimica Acta 1974, 304, 1125.
- 66. Brown, M. P.; Heseltine, R. W. Chem. Commun. 1968, 1551.
- 67. Brown, M. P.; Heseltine, R. W.; Smith, P. A.; Walker, P. J. J. Chem. Soc. A 1970, 410.
- 68. Shubina, E. S.; Bachmutova, E. V.; Saitkulova, L. N.; Epstein, L. M. Mendeleev Commun. 1997, 83.
- 69. Epstein, L. M.; Shubina, E. E.; Bakhumotva, E. V.; Saitkilova, L. N.; Bakhumutov, V. L.; Chistyakov, A. L.; Stankevich, I. V. *Inorg. Chem.* 1998, 37, 3013.
- 70. Shubina, E. S.; Belkova, N. V.; Bakhmutova, E. V.; Saitkulova, L. N.; Ionidis, A. V.; Epstein, L. M. Russ. Chem. Bull. 1998, 47, 817.
- 71. Jackson, J. E.; Huang, R.; Eckert, J.; Sharma, M.; Argyriou, D.; Sheldon, R. Manuscript in preparation.
- 72. Richardson, T. B.; de Gala, S.; Crabtree, R. H. Siegbahn, P. E. M. J. Am. Chem. Soc. 1995, 117, 12875.
- 73. Cramer, C. J.; Gladfelter, W. L. Inorg. Chem. 1997, 36, 5358.
- 74. Klooster, W.T.; Koetzle, T. F.; Siegbahn, P. E. M.; Richardson, T. B.; Crabtree, R. H. J. Am. Chem. Soc. 1999, 121, 6337.
- 75. Singh, P.; Zottola, M.; Huang, S.; Show, B. R.; Pedersen, L. G. Acta Cryst. 1996, C52, 693.
- 76. Popelier, P. L. A. J. Phys. Chem. A 1998, 102, 1873.

- 77. Rozas, I.; Alkorta, I.; Elguero, J. Chem. Phys. Lett. 1997, 275, 423.
- 78. Alkorta, I.; Elguero, J.; Foces-Foces, C. J. Chem. Soc. Commun. 1996, 1633.
- 79. Crabtree, R. H.; Siegbahn, P. E. M.; Eisenstein, O. Rheingold, A. L.; Koetzle, T. F. Acc. Chem. Res. 1996, 29, 348.
- 80. Atwood, J. L.; Koutsantonis, G. A.; Lee, F.-C.; Raston, C. L. *Chem. Comm.* 1994, 91.
- 81. Campbell, J. P.; Hwang, J. W.; Young, V. G.; Von Dreele, R. B.; Cramer, C. J.; Gladfelter, W. L. J. Am. Chem. Soc. 1998, 120, 521.
- 82. Liu, Q.; Hoffmann, R. J. Am. Chem. Soc. 1995, 117, 10108.
- 83. Alkorta, I.; Elguero, J.; Foces-Foces, C. Chem. Commun. 1996, 1633.
- 84. Remko, M. Molecular Physics 1998, 94, 839.
- 85. Kulkarni, S. A. J. Phys. Chem. A. 1998, 102, 7704.
- 86. Kulkarni, S. A.; Srivastava, A. K. J. Phys. Chem. A 1999, 103, 2836.
- 87. Lundell, J.; Petersson, M. Phys. Chem. Chem. Phys. 1999, 1, 1601.
- 88. Grabowski, S. J. Chem. Phys. Lett. 1999, 312(5-6), 542.
- 89. Grabowski, S. J. J. Phys. Chem. A 2000, 104, 5551.
- 90. Stevens, R.; Bau, R.; Milstein, D.; Blum, O.; Koetzle, T. F. J. Chem. Soc. Dalton Trans 1990, 1429.
- 91. Park, S.; Ramachandran, R.; Lough, A. J.; Morris, R. H. J. Chem. Soc. Chem. Commun. 1994, 2201.

- 92.Lee, J. C.; Rheingold, A. L.; Miller, B.; Pregosin, P. S.; Crabtree, R. H. Chem. Commun. 1994, 2001.
- 93. Peris, E.; Lee, J. C.; Rambo, J. R.; Eisenstein, O.; Crabtree, R. H. J. Am. Chem. Soc. 1995, 117, 3485.
- 94.Lough, A. J.; Park, S.; Ramachandran, R.; Morris, R. H. J. Am. Chem. Soc. 1994, 116, 8356.
- 95. Park, S.; Lough, Morris, R. H. Inorg. Chem. 1996, 35, 3001.
- 96. Wessel, J.; Lee, J. C.; Peris, E.; Yap, G. P. A.; Fortin, J. B.; Ricci, J. S.; Sini, G.; Albinati, A.; Koetzle, T. F.; Eisenstein, O.; Rheingold, A. L.; Crabtree, R. H. Angew. Chem. Int. Ed. 1995, 34, 2507.
- 97. Patel, B. P.; Wessel, J.; Yao, W.; Lee Jr., J. C.; Peris, E.; Koetzle, T. F.; Yap, G. P. A.; Fortin, J. B.; Ricci, J. S.; Sini, G.; Albinati, A.; Eisenstein, O.; Rheingold, A. L.; Crabtree, R. H. New J. Chem. 1997, 21, 413.
- 98. Sini, G.; Eisenstein, O.; Yao, W.; Crabtree, R. H. *Inorg. Chim. Acta* 1998, 280, 26.
- 99. Peris, E.; Wessel, J.; Patel, B. P.; Crabtree, R. H. Chem. Commun. 1995, 2175.
- 100.Desmurs, P.; Kavallieratos, K.; Yao, W.; Crabtree, R. H. *New J. Chem.* **1999**, *23*, 1111.
- 101. Shubina, E. S.; Belkova, N. V.; Krylov, A. N.; Vorontsov, E. V.; Epstein, L. M.; Gusev, D. G.; Niedermann, M.; Berke, H. J. Am. Chem. Soc. 1996, 118, 1105.
- 102.Belkova, N. V.; Shubina, E. S.; Ionidis, A. V.; Epstein, L. M.; Jacobsen, H.; Messmer, A.; Berke, H. *Inorg. Chem.* 1997, 36, 1522.
- 103. Messmer, A.; Jacobsen, H.; Berke, H. Chem. Eur. J. 1999, 5, 3341.

- 104. Scheiner, S.; Orlova, G. J. Phys. Chem. A 1998, 102, 260.
- 105.Cremer, D.; Kraka, E. J. Phys. Chem. 1986, 90, 33.
- 106.Matsunaga, N.; Gordon, M. S. J. Phys. Chem. 1995, 99, 12773.
- 107. Paulson, J. F.; Henchman, M. J. Bull. Am. Phys. Soc. 1982, 27, 108.
- 108.Miller, T. M.; Viggiano, A. A.; Stevens Miller, A. E.; Morris, R. A.; Henchman, M.; Paulson, J. F.; Van Doren, J. M. J. Chem. Phys. 1994, 100, 5706.
- 109.de Beer, E.; Kim, E. H.; Neumark, D. M.; Gunion, R. F.; Lineberger, W. C. J. Phys. Chem. 1995, 99, 13627.
- 110.Lee, J. C.; Peris, E.; Rheingold, A. L.; Crabtree, R. H. J. Am. Chem. Soc. 1994, 116, 11014.
- 111.Ayllon, J. A.; Gervaux, C.; Sabo-Etienne, S.; Chaudret, B. Organometallics 1997, 16, 2000.
- 112.Orlova, G.; Scheiner, S. J. Phys. Chem. Soc. 1994, 116, 11014.
- 113. Shubina, E. S.; Belkova, N. V.; Bakhmutova, E. V.; Vorontsov, E. V.; Bakhmutov, V. I.; Ionidis, A. V.; Bianchini, C.; Marvelli, L.; Peruzzini, M.; Epstein, L. M. *Inorg. Chim. Acta* 1998, 280, 302.
- 114. Epstein, L. M.; Shubina, E. S. Ber. Bunsenges. Phys. Chem. 1998, 102, 359.
- 115.Orlova, G.; Scheiner, S. J. Phys. Chem. A 1998, 102, 4813.
- 116.Grundemann, S.; Ulrich, S.; Limbach, H. –H.; Golubev, N. S.; Denisov, G. S.; Epstein, L. M.; Sabo-Etienne, S.; Chaudret, B.; *Inorg. Chem.* 1999, 38, 2550.
- 117.Chu, H. S.; Lau, C. P.; Wong, K. Y.; Wong, W. T. Organometallics 1998, 17, 2768.
- 118. Musashi, Y.; Sakaki, S. J. Am. Chem. Soc. 2000, 122, 3867.

- 119. Yamakawa, M.; Ito, H.; Noyori, R. J. Am. Chem. Soc. 2000, 122, 1466.
- 120. Abdur-Rashid, K.; Faatz, M.; Lough, A.; Morris, R. H. J. Am. Chem. Soc. 2001, 123, 7473.
- 121. Ayllon, J. A.; Sayers, S. F.; Sabo-Etienne, S.; Donnadieu, B.; Chaudret, B. Organometallics 1999, 18, 3981.
- 122. Caballero, A.; Jalon, F. A.; Manzano, B. R. Chem. Commun. 1998, 1879.
- 123. Abdur-Rashid, K.; Gusev, D. G.; Lough, A. J.; Morris, R. H. Organometallics, 2000, 19, 834.
- 124. Patel, B. P.; Kavallieratos, K.; Crabtree, R. H. J. *Organomet. Chem.* 1997, 528, 205.
- 125.Bosque, R.; Maseras, F.; Eisenstein, O.; Patel, B. P.; Yao, W.; Crabtree, R. H. *Inorg. Chem.* 1997, 36, 5505.
- 126. Yao, W.; Crabtree, R. H. Inorg. Chem. 1996, 35, 3007.
- 127. Aime, S.; Gobetto, R.; Valls, E. Organometallics 1997, 16, 5140.
- 128.Aime, S.; Ferriz, M.; Gobetto, R.; Valls, E. Organometallics 1999, 18, 2030.
- 129. Aime, S.; Ferriz, M.; Gobetto, R.; Valls, E. Organometallics 2000, 19, 707.
- 130.Gatling, S. C.; Jackson, J. E. J. Am. Chem. Soc. 1999, 121, 8655.
- 131. Custelcean, R.; Jackson, J. E. J. Am. Chem. Soc. 2000, 122, 5251.
- 132.Mesmer, R. E.; Jolly, W. L. Inorg. Chem. 1962, 1, 608.
- 133. Schreiner, P.R.; Schaefer, H. F.; Schleyer, P. von Rague J. Chem. Phys. 1995, 103, 5565.

- 134. Cukier, R. I.; Zhu, J. J. Chem. Phys. 1999, 110, 9587.
- 135. Webb, S. P.; Iordanov, T.; Hammes-Schiffer, S. J. Chem. Phys. **2002**, 117, 4106.
- 136. Private communication with Professor S. Hammes-Schiffer.
- 137.Davis, R. E. J.Am. Chem. Soc. 1962, 84, 892.
- 138.Kreevoy, M. M.; Hutchins, J. E. C. J. Am. Chem. Soc. 1969, 91, 4329.
- 139. Prepperberg, I. M.; Halgren, T. T.; Lipscomb, W. N. J. Am. Chem. Soc. 1976, 98, 3442.
- 140.Garrett, E. R.; Lyttle, D. A. J. Am. Chem. Soc. 1953, 75, 6051.
- 141. Wigfield, D. G.; Gowland, F. W. Can. J. Chem. 1976, 56, 786.
- 142.Personal communication with dr. S. Gatling
- 143.Henderson, W. G.; How, M. J.; Kennedy, G. R.; Mooney, E. F. Carbohydrate Res. 1973, 28, 1.
- 144.Frisch, M. J.; Trucks, G. W.; Schlegel, H. B.; Gill, P. M. W.; Johnson, B. G.; Robb, M. A.; Cheeseman, J. R.; Keith, T. A.; Peterson, G. A.; Montgomery, J. A.; Raghavachari, K.; Al-Laham, M. A.; Zakrzewski, V. G.; Ortiz, J. V.; Foresman, J. B.; Cioslowski, J.; Stefanov, B. B.; Nanayakkara, A.; Challacombe, M.; Peng, C. Y.; Ayala, P. Y.; Chen, W.; Wong, M. W.; Andres, J. L.; Replogle, E. S.; Gomperts, R.; Martin, R. L.; Fox, D. J.; Binkley, J. S.; Defrees, D. J.; Baker, J.; Steward, J. P.; Head-Gordon, M.; Gonzales, C.; Pople, J. A. Gaussian 94 (Revision D.3); Gaussian, Inc.: Pittsburgh, PA, 1995.
- 145.Frisch, M. J.; Trucks, G. W.; Schlegel, H. B.; Scuseria, G. E.; Robb, M. A.; Cheeseman, R.; Zakrzewski, J. R. V. G.; Montgomery Jr., J. A.; Stratmann, R. E.; Burant, J. C.; Dapprich, S.; Millam, J. M.; Daniels, A. D.; Kudin, K. N.; Strain, M. C.; Farkas, O.; Tomasi, J.; Barone, V.; Cossi, M.; Cammi, R.; Mennucci, B.; Pomelli, C.;

Adamo, C; Clifford, S.; Ochterski, J.; Petersson, G. A.; Ayala, P. Y.; Cui, Q.; Morokuma, K.; Salvador, P.; Dannenberg, J. J.; Malick, D. K; Rabuck, A. D.; Raghavachari, K.; Foresman, J. B.; Cioslowski, J.; Ortiz, J. V.; Baboul, A. G.; Stefanov, B. B.; Liu, G.; Liashenko, A.; Piskorz, P.; Komaromi, I.; Gomperts, R.; Martin, R. L.; Fox, D. J.; Keith, T.; Al-Laham, M. A.; Peng, C. Y.; Nanayakkara, A.; Challacombe, M.; Gill, P. M. W.; Johnson, B.; Chen, W.; Wong, M. W.; Andres, J. L.; Gonzalez, C.; Head-Gordon, M.; Replogle, E. S.; Pople, J. A. *Gaussian 98* (Revision A.11.1); Gaussian, Inc.: Pittsburgh, PA, 2001.

- 146.Schmidt, M. W.; Baldridge, K. K.; Boatz, J. A.; Elbert, S. T.; Gordon, M. S.; Jensen, J. J.; Koseki, S.; Matsunaga, N.; Nguyen, K. A.; Su, S.; Windus, T. L.; Dupuis, M.; Montgomery, J. A. J. Comput. Chem. 1993, 14, 1347.
- 147. Taketsugu, T.; Gordon, M. S. J. Chem. Phys. 1995, 103, 10042.
- 148.Dr. S. Gatling thesis

